UNCLASSIFIED

AD NUMBER
ADC025992
CLASSIFICATION CHANGES
TO: unclassified
FROM: confidential
LIMITATION CHANGES
TO: Approved for public release, distribution unlimited
FROM: Controlling DoD Organization: Naval Electronic Systems Command, Washington, DC 20360.
AUTHORITY
ONR ltr, 31 Jan 2006; ONR ltr, 31 Jan 2006

THIS PAGE IS UNCLASSIFIED

CONFIDENTIAL

NOSC

NOSC TR 664

AD C025992

Technical Report 664

ARRAY SIMULATION AT THE BEARING STAKE SITES (U)

DF Gordon

April 1981

Final Report: September 1979–April 1981

Prepared for
Naval Electronic Systems Command

DTIC ELECTE SEP 9 1981 S D A

DTIC FILE COPY

Classified by: OPNAVINST S5513.5-03
Review on: 31 December 1995

"NATIONAL SECURITY INFORMATION"
"Unauthorized Disclosure Subject to Criminal Sanctions"

NAVAL OCEAN SYSTEMS CENTER
SAN DIEGO, CALIFORNIA 92152

CONFIDENTIAL

81 9 08 504

NAVAL OCEAN SYSTEMS CENTER, SAN DIEGO, CA 92152

AN ACTIVITY OF THE NAVAL MATERIAL COMMAND

SL GUILLE, CAPT, USN
Commander

HL BLOOD
Technical Director

ADMINISTRATIVE INFORMATION (U)

(U) This report was prepared under a subtask of the FY 79 NOSC Block Program in Environmental Acoustic Surveillance Technology, PE 62759, XF-59-552, sponsored by the Naval Electronic Systems Command, Code 320.

Released by
MR Akers, Head
Systems Concept and
Analysis Division

Under authority of
EB Tunstall, Head
Surveillance Systems Department

ACKNOWLEDGEMENTS (U)

(U) Dr JA Newbert, J Ambros, and PW Schey made the array analysis program available and assisted in problems of input format. Dr ER Floyd assisted in computational work and reviewed the report. MA Pedersen gave advice and guidance during the work and also reviewed the report.

CONFIDENTIAL

SECURITY CLASSIFICATION OF THIS PAGE (When Data Entered)

(14) REPORT DOCUMENTATION PAGE		READ INSTRUCTIONS BEFORE COMPLETING FORM
1. REPORT NUMBER NOSC/TR-664 NOSC Technical Report 664 (TR 664)	2. GOVT ACCESSION NO. AD-C025	3. RECIPIENT'S CATALOG NUMBER 992
4. TITLE (and Subtitle) (6) ARRAY SIMULATION AT THE BEARING STAKE SITES. (U)		5. TYPE OF REPORT & PERIOD COVERED (9) Final Report, Sept 1979 - April 1981
		6. PERFORMING ORG. REPORT NUMBER
7. AUTHOR(s) DF Gordon (10) D. F. Gordon		8. CONTRACT OR GRANT NUMBER(s) 12 46
9. PERFORMING ORGANIZATION NAME AND ADDRESS Naval Ocean Systems Center San Diego, CA 92152		10. PROGRAM ELEMENT, PROJECT, TASK AREA & WORK UNIT NUMBERS PE 62759 XF-59-552
11. CONTROLLING OFFICE NAME AND ADDRESS Naval Electronic Systems Command Washington, DC 20360		12. REPORT DATE April 1981
		13. NUMBER OF PAGES 41
14. MONITORING AGENCY NAME & ADDRESS (if different from Controlling Office) (17) F59552		15. SECURITY CLASS. (of this report) Confidential
		15a. DECLASSIFICATION/DOWNGRADING SCHEDULE Review on: 31 December 1995

16. DISTRIBUTION STATEMENT (of this Report)

17. DISTRIBUTION STATEMENT (of the abstract entered in Block 20, if different from Report)

18. SUPPLEMENTARY NOTES

19. KEY WORDS (Continue on reverse side if necessary and identify by block number)

Acoustic arrays	LATA
Long arrays	OAMS
Bearing Stake	Array simulation
	Array tilt

20. ABSTRACT (Continue on reverse side if necessary and identify by block number)

(C) Acoustic pressures were computed at range-depth points to simulate narrowband, low frequency data (gathered by two long towed arrays), LATA, and OAMS. The pressures were computed with a normal mode program using environmental conditions that were observed during the Bearing Stake exercises. These data were processed by the same computer program used to process recorded data from the exercise. Comparisons between the computed and observed data indicate that a 1.5 degree tilt in LATA resulted in about 0.5 dB loss in array signal gain. A tilt of 1 degree in OAMS accounted for almost none of the observed loss. The loss in array signal gain of the computed data arises when multipath interference nulls occur at the array location.

DD FORM 1473, 1 JAN 73 EDITION OF 1 NOV 65 IS OBSOLETE

S/N 0102-LF-014-6601

CONFIDENTIAL

SECURITY CLASSIFICATION OF THIS PAGE (When Data Entered)

371 1-7

20. ABSTRACT (Continued)

This effect does not account for a major part of the observed loss. Serpentine oscillations which can be seen in plots of coherence between element pairs can be simulated from the computed data by adding a second source separated from the first by a few degrees in azimuth. Some simulations of small amplitude array deformation showed only minor effects.

OBJECTIVE (U)

(C) Determine the coherence and array signal gain for Long Acoustic Towed Array (LATA) and Ocean Acoustic Measurement System (OAMS) in a simulated sound field in the same way they were determined for observed Bearing Stake data. Find the effect of array tilt on array performance. Increase the utility of the Bearing Stake array coherence observations by isolating the cause of observed effects.

RESULTS (U)

1. (C) A tilt of 1.5 degrees in LATA causes an average of about 0.5 dB loss in array signal gain out of an average observed loss of over 2 dB.

2. (C) A tilt of 1.0 degree in OAMS causes an average of only 0.1 dB loss in array signal gain out of an average observed loss of 2 dB.

3. (U) Serpentine oscillations in the plots of coherence between array elements, can arise from a second arrival separated from the first by a few degrees in azimuth. An echo or a noisy ship is a possible source of such a second arrival.

4. (U) Sinusoidal array deformations of up to 4 m amplitude usually cause less than 0.2 dB loss in array signal gain at 25 Hz.

5. (U) Loss in array signal gain of over 2 dB is demonstrated at ranges where multipath nulls occur.

APPLICATION TO NAVY PROBLEMS (U)

1. (U) Performance loss due to array tilt for several cases in the Bearing Stake area is given herein. These losses can give guidance for extrapolating to other array tilt parameters.

2. (U) Some numerical data on performance loss due to array deformation are given herein.

3. (U) Operators and analysts are alerted to look for second sources when serpentine waves are observed in coherence plots.

4. (U) Array tilt is eliminated as a major cause of loss in array signal gain for OAMS at the Bearing Stake sites. Other explanations must be sought, eg, temporal fluctuations, array element failure, or array deformation.

RECOMMENDATIONS (U)

(U) Use beam patterns or exercise reconstructions to see if a source for a second signal can be identified in Site 4, Tow 4P1, as indicated by the serpentine coherence plots.

(U) Simulate arrays in three dimensions so array tilt, array projection in range, and array deformations can be evaluated in a multipath field. Determine the multipath limitation on coherence distances in the depth and range dimension. Compare these results from the Bearing Stake area with those from other ocean areas to determine the relative effects of the above variables in different sound propagation regimes.

CONTENTS (U)

ILLUSTRATIONS (U)

ILLUSTRATIONS (U) (Contd)

TABLES (U)

INTRODUCTION (U)

(C) During the Bearing Stake exercise[1] two towed arrays, the Ocean Acoustic Measurement System and the Long Acoustic Towed Array (OAMS and LATA), were operated in the northwestern Indian Ocean at five sites. Data from each hydrophone group, for both arrays, were stored on magnetic tape while a continuous wave source was being towed within a detectable range of the array. Portions of this data have been processed at NOSC to determine the amount of coherence in the signal along the array and the loss in array signal gain. These results have been published by Drs JA Neubert and AG Fabula.[1-4]

(U) A normal mode program has been used to interpret various observed propagation effects at the Bearing Stake sites.[5] This program can be used to compute sound fields which can be processed by the same program performing the array analysis. This simulation can determine the sources of some of the observed correlation or decorrelation along the array. These results are reported herein. The effect of array tilt in a sound field made inhomogenous by multipath effects is of particular interest. Some computations of the effects of array deformation are also reported here. The effect of the range projection of a long array in a multipath field is closely related to array tilt. Such effects have been modeled in previous work[6] but have not been done for the Bearing Stakes sites. In the current work all arrays are modeled broadside to the source so the range projection is zero.

---

1. Naval Ocean Systems Center TR 383, "Bearing Stake Coherence and Array Signal Gain Area Assessment Report (U)" by JA Neubert, Confidential, December 1978

2. Naval Ocean Systems Center TN 380, "Bearing Stake Coherence Data Analysis, OAMS Array (U)" by JA Neubert, Confidential, 6 February 1978*

3. Naval Ocean Systems Center TN 589, "Bearing Stake Coherence Data Analysis: LATA (U)" by AG Fabula and JA Neubert, Confidential, December 1978*

4. JA Neubert, "Coherence and Its Sound Field Structure in the Northwestern Indian Ocean (U)," JUA(USN) 30(3), p 367-398, Confidential, 1980

5. Naval Ocean Systems Center TR 467, "Propagation Loss Assessment of the Bearing Stake Exercise (U)" by MA Pederson and GS Yee, Confidential, September 1979

6. DF Gordon and ER Floyd, "Acoustic Propagation Effects in Beam Forming of Long Arrays (U)," JUA(USN) 29(1), p 1-16, Confidential, January 1979

*NOSC Technical Notes are informal publications intended primarily for use in the Center.

(U) In this report the two towed arrays and the experimental setup are described first. Next, the techniques for modeling this process are described. The array signal gain (ASG) for the modeled data is then compared to that for the observed data. A study of some anomalous serpentine waves in the experimental coherence plots is then reported.

EXPERIMENTAL CONFIGURATION (U)

(C) A source was towed at ranges up to 600 km from the arrays at depths of 80-95 m. A MK-6 projector was used for the frequencies from 20 to 25 Hz. Source level was 188 to 190 dB/ Pa. Tow tracks can be found in references 1 and 2. The cw source alternated between two frequencies, usually 22 and 25 Hz. The duration of each frequency was 5 or 10 minutes. A 4 minute sample was chosen within these intervals. In this report only frequencies of 22 and 25 Hz are modeled — other frequencies are reported in reference 2.

THE LATA ARRAY (U)

(C) The LATA array is 1200 m long with 64 hydrophone groups or elements evenly spaced at 19.05 m. The signal arriving from each group was digitized and stored on magnetic tape. A fast Fourier transform was performed on each 2048 samples (4 seconds of data); the signal was selected from the appropriate frequency bin to be used in the array analysis program.

(C) The array was generally towed at 300 m depth. Four depth sensors on the array gave depth and tilt. With the exception of Site 1B the array was estimated not to have over a 1.5 degree tilt. Over its 1200 m length this corresponds to a spread in element depths of 30 m. On the final station, Site 2, weights were added to the array to overcome its apparent buoyancy. The depth sensors failed on this run and the actual tilt is not known. Data to be discussed later suggest that the tilt was significantly reduced.

THE OAMS ARRAY (U)

(C) The OAMS array is 925.4 m in length. It has 32 hydrophone groups or elements spaced about the midpoint with density equal to a cosine function. Table 1 gives the depths of the elements assuming an array tilt of 1 degree with the deeper end at 200 m. The element spacing can be inferred from this table. The tilt of the OAMS array was estimated not to exceed 1 degree.

(C) OAMS data were processed by a quadrature method giving amplitude and phase of each sample and stored on magnetic tape. These samples were used in the array analysis program. The data from either array were thus analyzed by the same digital computer program. A sample was taken each 4 seconds for LATA and each 1 second for OAMS. The data were averaged for each hydrophone and coherence was computed for each pair of hydrophones. The average data for 4 minutes were beamformed for each 0.5 degree in azimuth and the direction of maximum response found. The ASG was calculated at this steering angle. A variety of statistical measures for the coherence of phase, amplitude, and the combination of both along with several types of beamforming are given in references 1-4. Here we will use the array signal gain, the average signal amplitude at each element, and the coherence versus element separation to compare to modeled results.

ARRAY PERFORMANCE SIMULATION (U)

(U) Normal mode theory gives the steady state acoustic pressure at any point in range and depth for the idealized boundary conditions. The pressure is a complex number which gives both absolute value and phase of the pressure relative to that at unit distance from a unit source. Modeling the experimental results is then just a matter of computing pressure at the range and receiver depth of each element at the time a sample is observed. These values are then processed with the same program as were the observed data. The output should reflect the parameters included in the model.

ARRAY TILT (U)

(C) In the current work we place the target broadside to the array. It is assumed that the slant range to different elements is negligible. The range change between samples represents a given range rate between source and array. Receiver depths vary progressively along the array due to array tilt. For the equally spaced elements of the LATA array the 1.5 degree tilt gives 0.476-m depth between elements. Table 1 gives the depths for the unequally spaced elements of the OAMS array at a tilt of 1 degree.

Element No	Depth (m)	Element No	Depth (m)
1	185.00	17	192.93
2	185.80	18	193.21
3	186.54	19	193.52
4	187.24	20	193.84
5	187.90	21	194.19
6	188.52	22	194.57
7	189.10	23	194.99
8	189.63	24	195.45
9	190.12	25	195.95
10	190.58	26	196.48
11	191.00	27	197.05
12	191.38	28	197.67
13	191.73	29	198.33
14	192.06	30	199.03
15	192.36	31	199.78
16	192.65	32	200.57

(CONFIDENTIAL)

(C) Table 1. OAMS element depths with 1 degree tilt as used in the model.

COMPUTING THE SOUND PROPAGATION (U)

(U) The normal mode program used here is reported in reference 7. The sound speed profiles are taken from the representative sound speeds of reference 8 which were observed during the exercise. Figure 1 shows the profile

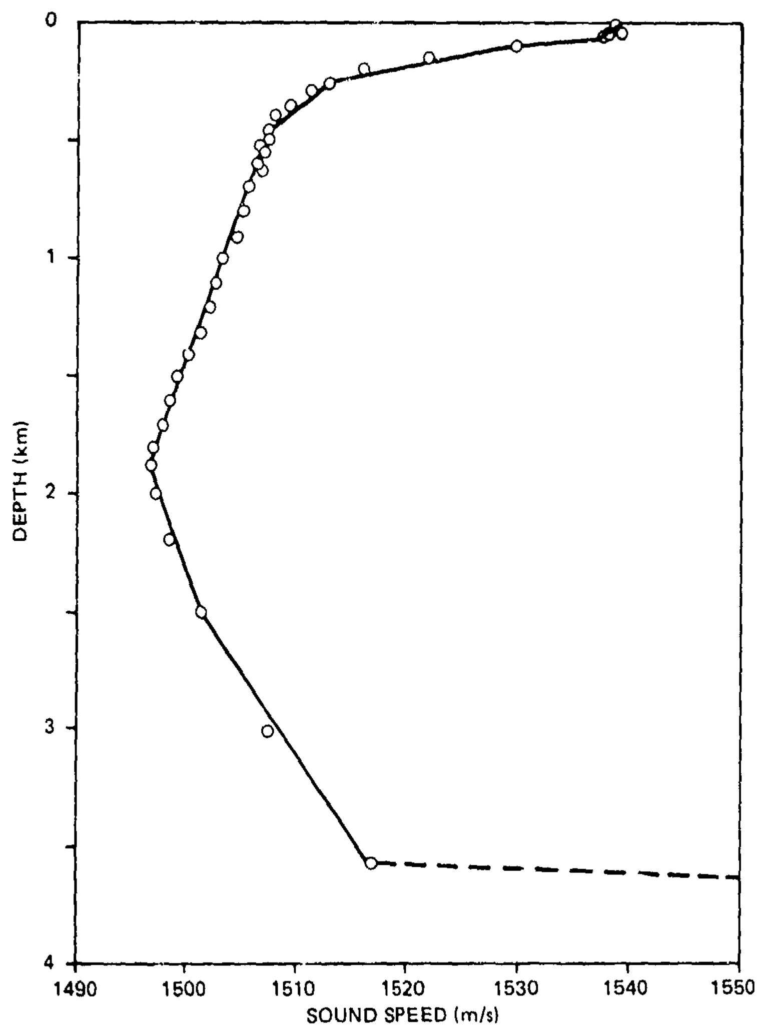

(UNCLASSIFIED)

(U) Figure 1. Sound speed profile for Site 3 (circles) with fitted layers in water (lines) and sediment (broken line).

---

7. Naval Ocean Systems Center TR 393, "Underwater Sound Propagation-Loss Program, Computation by Normal Modes for Layered Oceans and Sediments" by DF Gordon, Unclassified, May 1979

8. NORDA Report 18, "Bearing Stake Exercise: Sound Speed and Other Environmental Variability (U)" by DF Fenner and WJ Cronin, Jr, Confidential, September 1978

for Site 3 and the seven layer approximation to it used in the normal mode program. The sediment is also modeled as additional fluid layers — the first of which is shown in figure 1. Table 2 gives the sediment properties as given in reference 9. Those layers marked with asterisks are used in the model.

SITE 3

		Depth (m)	Sound Speed (m/s)	Attenuation (dB/m - kHz)	Density (gm/cm^3)
Water	*	0.0	1516.5	0	1.04373
Sediment	*	0	1517	0.0200	1.56
	*	100	1635	0.0098	1.65
		200	1737	0.0162	1.77
	*	300	1855	0.0220	1.90
		400	1959	0.0163	2.02
		500	2058	0.0103	2.10
		600	2153	0.0093	2.14
		700	2245	0.0085	2.17
		800	2332	0.0079	2.21
		900	2417	0.0073	2.24
	*	1000	2498	0.0069	2.27
		1500	2863	0.0062	2.38
		2000	3177	0.0062	2.47
		2500	3467	0.0062	2.53
		3000	3758	0.0062	2.58
	*	3260	3918	0.0062	2.60
Substrate	*	3260	5400	0.02	2.72

*These layers are used in the normal mode model.

(CONFIDENTIAL)

(C) Table 2. Sediment parameters for Site 3 as given by reference 9.

---

9. ARL-TR-79-24, "Analysis of Acoustic Bottom Interaction in Bearing Stake (U)," SK Mitchell and others, Confidential, February 1979

The sound speeds and absorption are continuous from layer to layer except at the top and bottom of the sediment where they are purposely made discontinuous. Densities are constant in each layer and are not necessarily continuous at interfaces.

(U) To save computer time and space the number of layers is kept as small as possible consistent with accurate modeling of the profile. Accurate modeling of the first 100 m of sediment is found to be most important in obtaining accurate reflection coefficients at low grazing angles. This is the reason for the particular choice of layers used in the sediment.

LATA SIMULATION RESULTS (U)

(C) In reference 3 coherence results from Site 4 are given in considerable detail. Site 4 was also modeled in more detail than other sites and is a good introductory case. This site, in the Somali Basin, is the only Bearing Stake site with bottom excess. This excess is slight but may permit some convergence zone effect at 25 Hz; it certainly would at higher frequencies. Site 4 is not typical of the other sites.

(U) Figure 2 compares the ASG for observed data at Site 4 to the computed data. The ASG is a negative number – this means that it represents a degradation in signal gain due to an imperfect sound field at the array elements. In the modeling, the 4 second samples were placed 10 m apart – this represents a range rate of 4.9 knots. This rate is consistent with the tow being modeled, Tow 4P1. The ASG is that for unweighted beamforming. For the weighted beamforming the ASG is similar but differs in detail.

(C) The average ASG for the data is 2.4 dB and for the computed propagation 0.7 dB. We conclude that 29 percent of the decibel loss in ASG is due to array tilt and different multipath structures at the various depths of the elements. Other sources of the observed loss in ASG are differing multipath structures at different ranges for sources off broadside, array deformation, noise interference, imperfect array elements, and spatial and temporal fluctuations. Noise interference is small in this case because the signal-to-noise ratio is over 20 dB. This report will show that at the bottom limited sites the ratio of simulated to observed loss is less than the 29 percent.

(U) The simulated results can be understood from a propagation loss plot. Figure 3 shows contours of propagation loss in an area 60 m in depth and 8 km in length. The rectangles represent individual determinations of ASG. The width is the range interval traveled during the 4 minute averaging time. The height is the depth interval over which the elements of the tilted array are distributed. The ASG is marked in each rectangle. Figure 3 suggests that loss in ASG results when nulls or high loss regions occur in the rectangles. Loss also occurs when elements at one depth experience a different loss structure than at another depth.

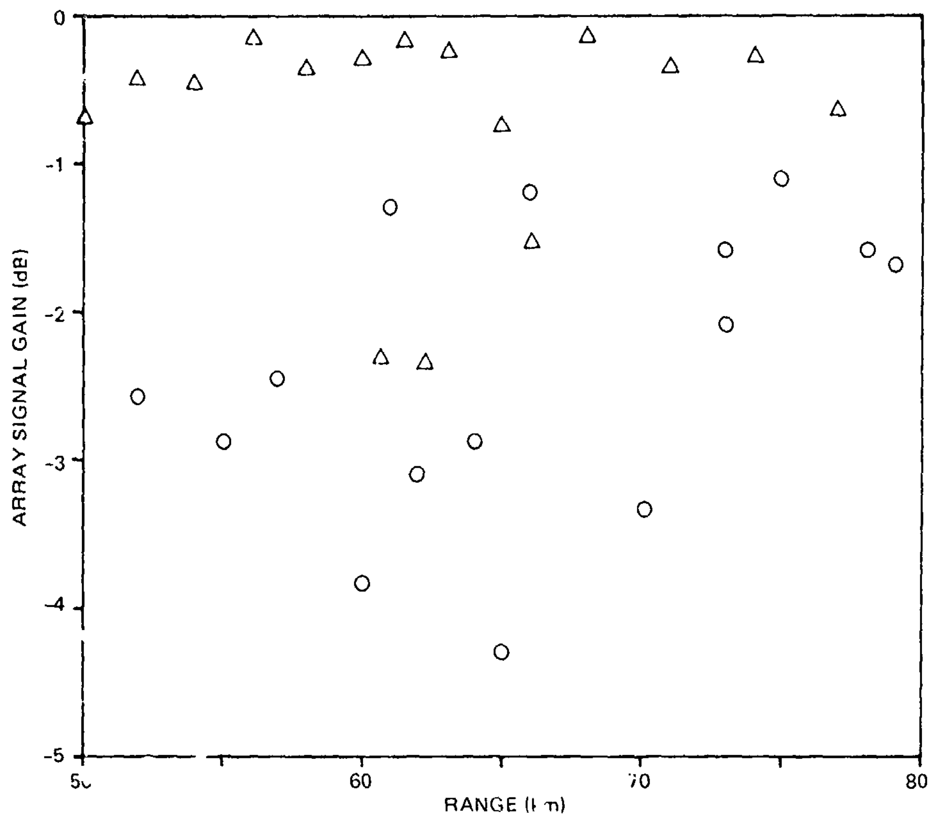

(CONFIDENTIAL)

(U) Figure 2. Array signal gain at ranges where observed data (o) and computed data (Δ) were processed for Site 4, 25 Hz, LATA. Some observed values are for 20 Hz.

(U) The rectangle extending from 62.5 to 63.1 km represents the array sample with greatest loss in AS3. Several plots developed by the array analysis program are shown for this worst case in figures 4–6. Several symbols on these plots (D, Ø, and AJ) are defined in reference 1–3 but are not used in this report. Figure 4 shows the array beam pattern for an unweighted array. The maximum signal is at 89.1 degrees or 0.9 degree off the true bearing of the signal. This is a distortion due to the irregularity of the signal and not to tipping the beam due to array tilt. This tipping could amount to 1/2 degree for rays arriving at 20 degrees from the horizontal. However, the tipping is of opposite sign for arrivals above and below the horizontal and the effects tend to cancel each other.

(C) Figure 5 shows the average propagation loss at each receiver depth as averaged across the 60 range steps. The horizontal axis title, "Sensor Group Separation," refers to position along the array. It is equivalent to our simulated receiver depth with shallower receivers at the left. The variation along the array can readily be correlated with the propagation loss contours of figure 3. This smooth curve is in sharp contrast to the equivalent curves

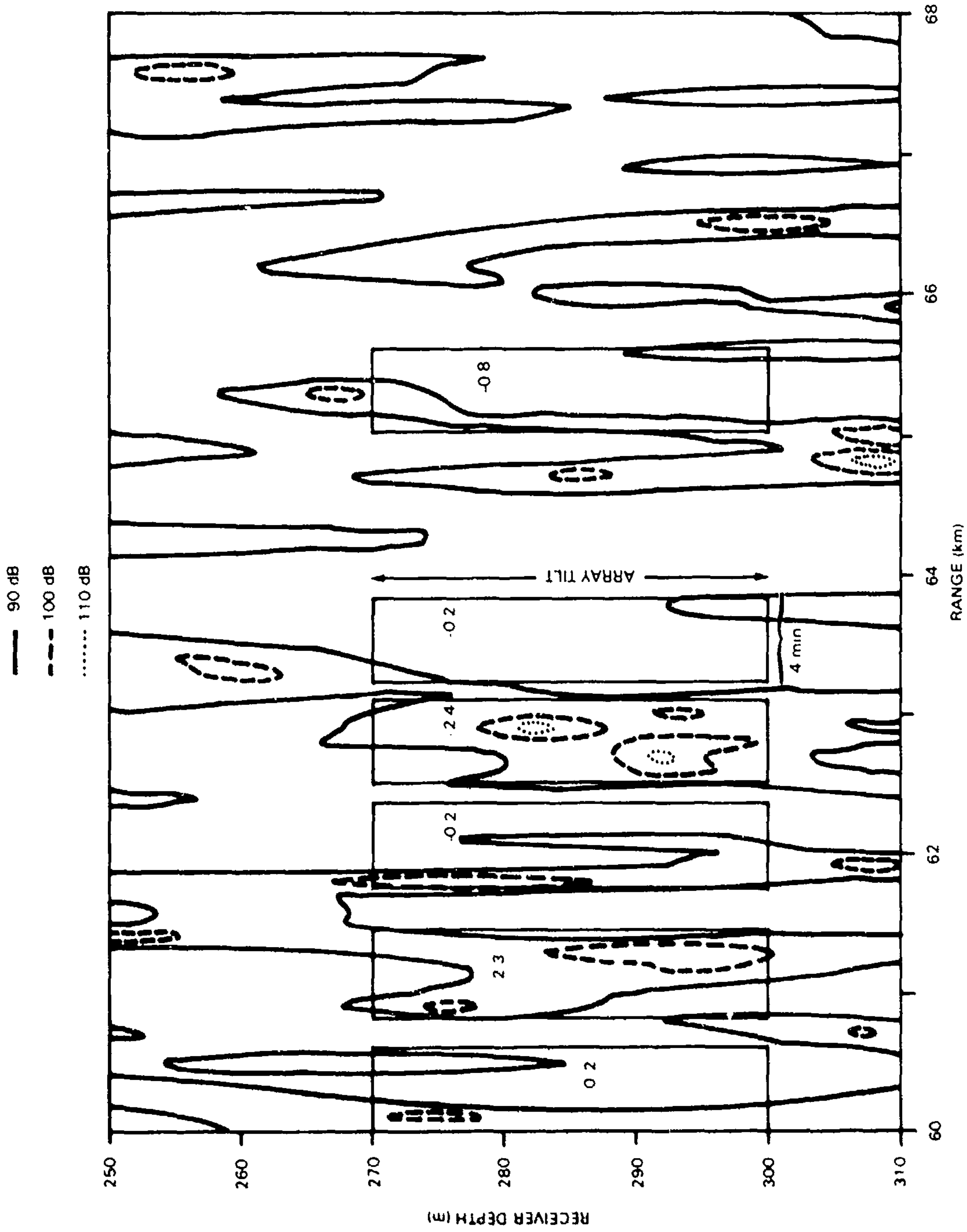

(UNCLASSIFIED)

(U) Figure 3. Propagation loss contours for Site 4, 25 Hz. Each rectangle shows the area covered by a single 4 minute tilted array sample.

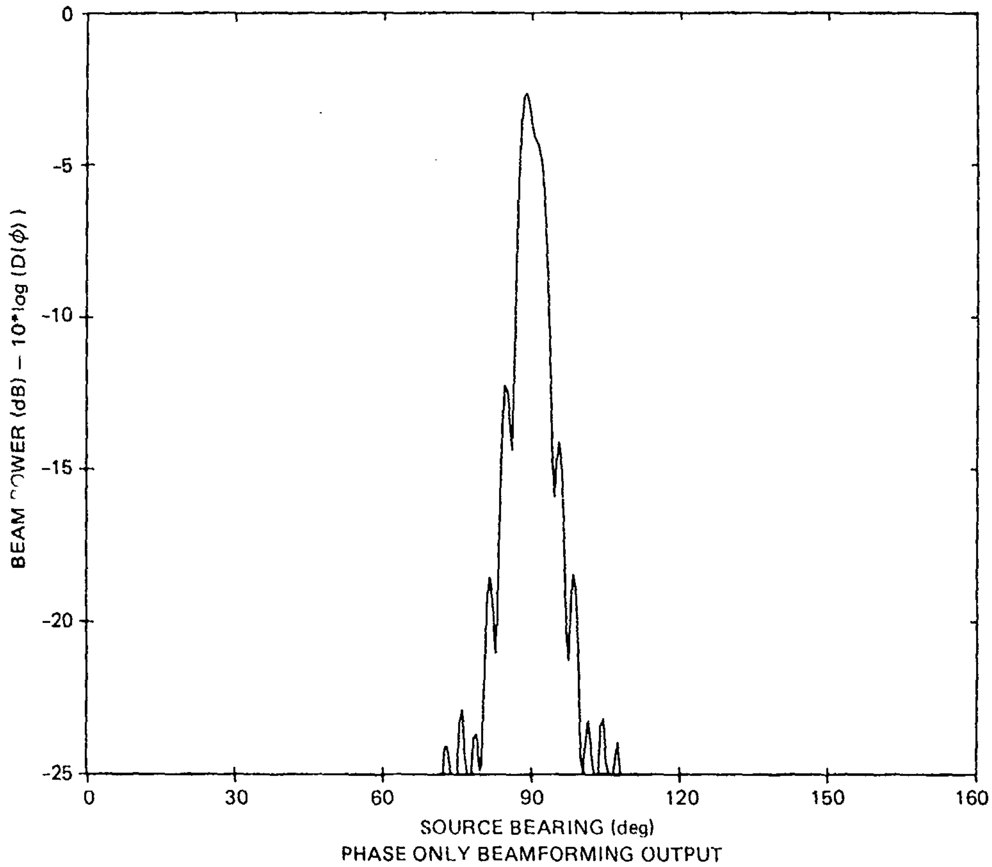

(UNCLASSIFIED)

(U) Figure 4. Beam pattern for computed sound field starting at range 62.5 km, Site 4. Unweighted beamforming is used here.

of the actual data. The curves shown in reference 2 and 3 and in figure 15 (of this report) have a consistent difference between hydrophone groups of from 5 to 10 dB for both arrays. This does not include some obviously bad groups which were omitted from the data.

(U) Figure 6a is a plot of coherence between receiver elements as a function of receiver separation along the array. Each dot represents the coherence between some pair of receivers computed over the 4 minute time (range) interval. This coherence plot resembles plots developed from the observed data although it is somewhat more regular. See reference 3, pages 88-91, and figure 13. This was a worst case. For most computed samples with ASG closer to 0 the coherence stays close to 1 for all element separations.

(U) Figure 6b shows the coherence of phase only between the elements as defined in reference 3. The irregularities in this figure arise because phase can be nearly discontinuous near null points. Because of this behavior we prefer the classical coherence which treats the complete complex number and not phase or amplitude separately. All three types are available in the array

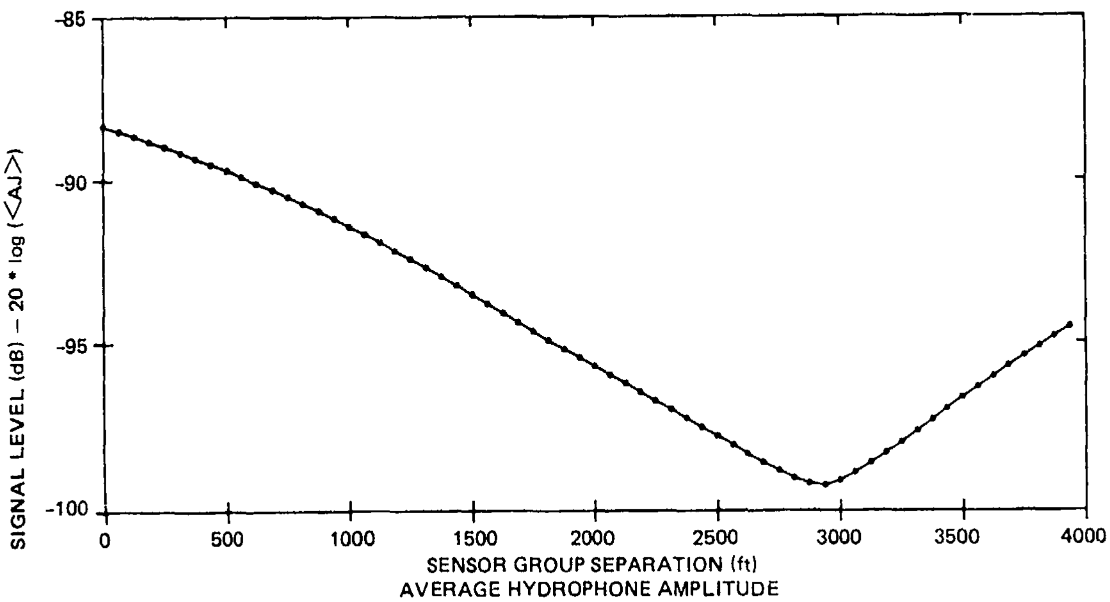

(UNCLASSIFIED)

(U) Figure 5. Average sound pressure amplitude over the 60 range samples (4 minute average) for each array element for the computed sound field starting at range 62.5 km.

analysis program. However, the classical coherence of figure 6a will be employed in this report.

(U) Many of the coherence plots for the observed data show a definite serpentine or sine wave effect. Further on we discuss attempts at modeling this sine wave effect. Arrival of a second signal, possibly an echo, can cause such results.

(U) The general shape of the collection of points in figure 6 can be interpreted from the loss contours of figure 3. The plot is for the fourth rectangle in figure 3 which contains two prominent nulls. The points with lowest coherence are for pairs for which one element passes near one of the nulls. The recovery in coherence at larger receiver separations is due to element pairs from above and below the nulls where the field is relatively unperturbed.

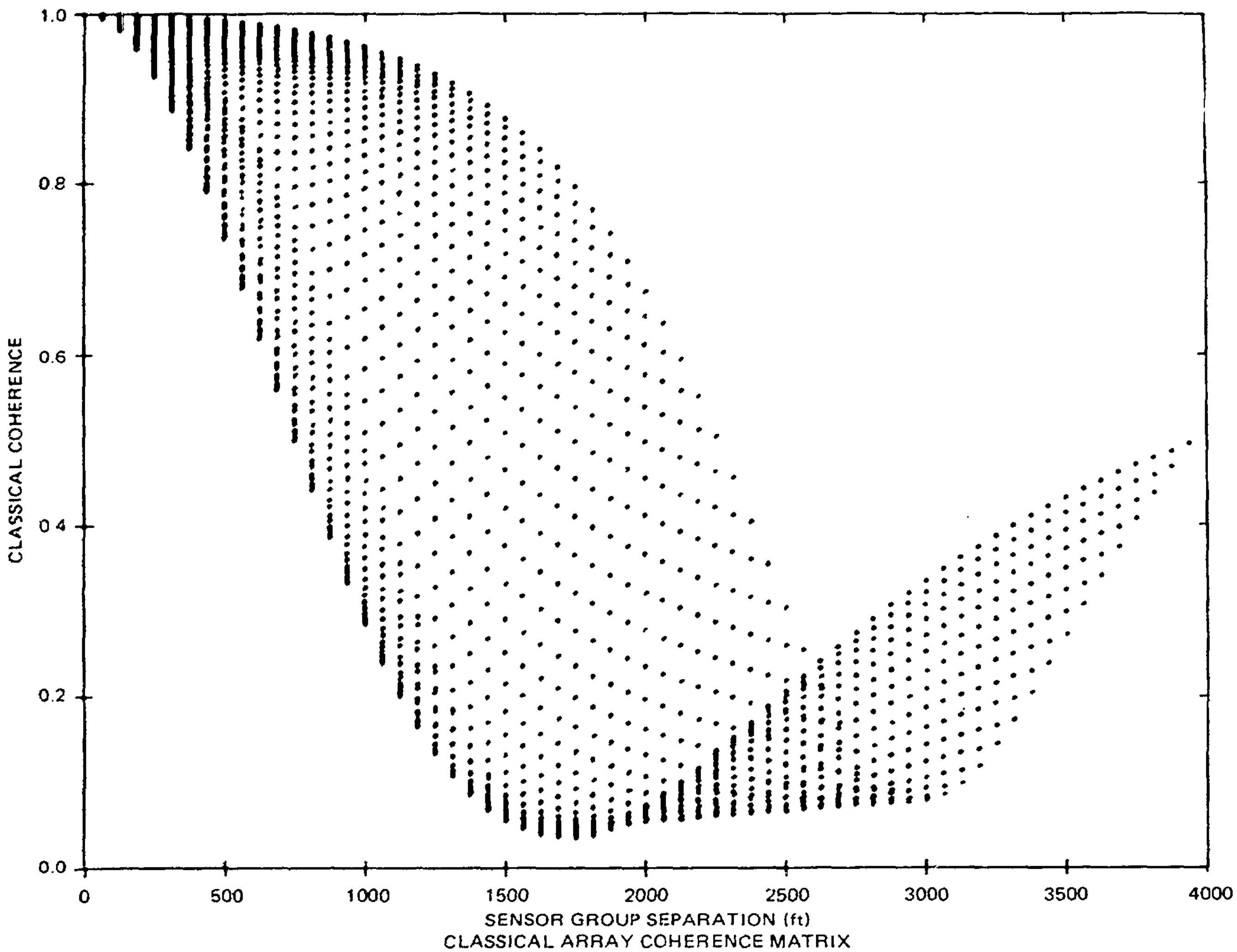

(UNCLASSIFIED)

(U) Figure 6a. Coherence between each pair of array elements over the 60 range samples plotted as a function of element separation. This plot is for the computed sound field starting at range 62.5 km.

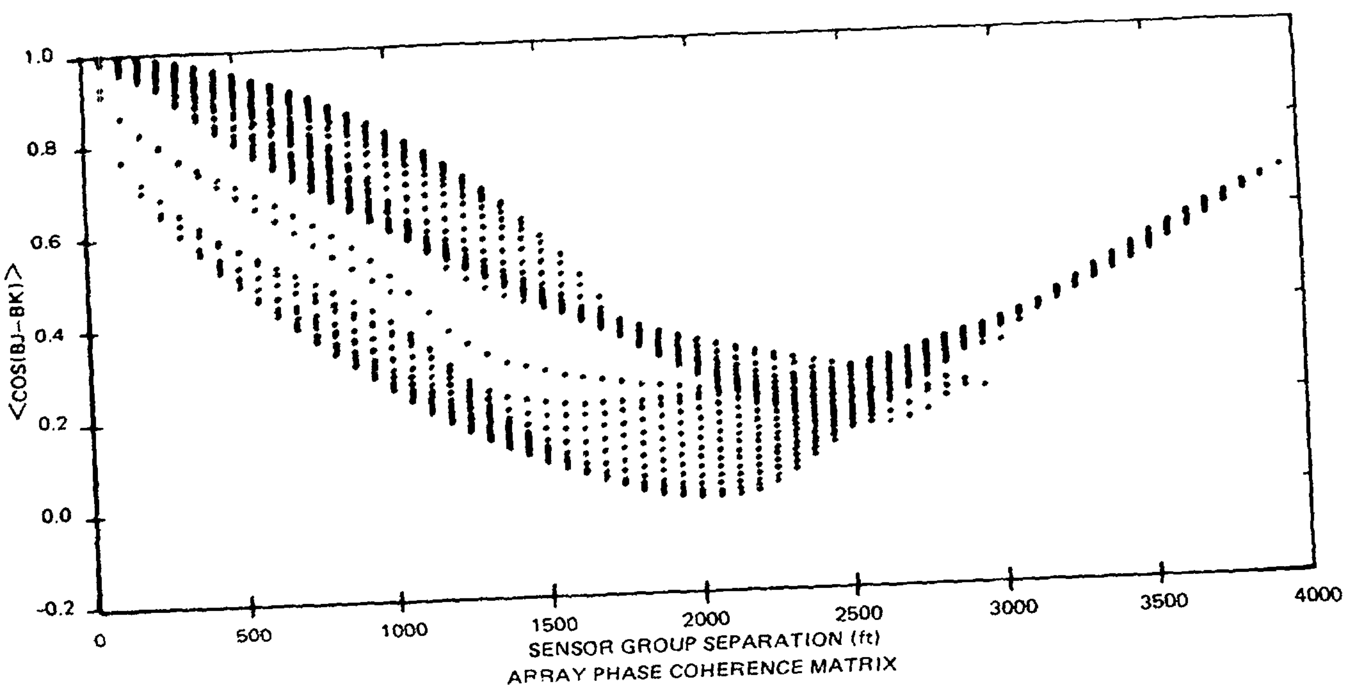

(UNCLASSIFIED)

(U) Figure 6b. Coherence between each pair of array elements over the 60 range samples plotted as a function of element separation. Phase only - not complete pressure consisting of phase and amplitude.

AVERAGING TIME (U)

(U) The computed samples are averaged here over 60 range steps which correspond to the 4 minute averaging time of the observed data. The effect of this range interval on ASG is of interest. To investigate this effect we ran three cases averaging over each 12 range steps and compared the results with the total range interval. This is equivalent to 120 m rather than a 600 m range change. These cases are compared with the longer averaging length in table 3. The first two sets cover range intervals where the sound fields are irregular and have significant losses in ASG. The third set is from a smooth area with negligible loss in ASG. For the first two sets the ASG for the total interval is less than that for every individual subinterval. For the third set, the ASG for the total interval equals the average for the subintervals. It is apparent from this that in an area where the sound field is irregular and contains nulls, the correlation distance in range is less than 600 m. In areas where the sound field is smooth, 600 m does not exceed the correlation distance.

Range		60.85 km	66.0 km	68.0 km
Segment	1	-1.09 dB	-0.85 dB	-0.12 dB
	2	-0.50	-0.80	-0.27
	3	-1.04	-1.32	-0.41
	4	-1.29	-0.81	-0.04
	5	-0.31	-0.88	-0.01
Average		-0.85	-0.93	-0.17
TOTAL		-2.176	-1.53	-0.17

(UNCLASSIFIED)

(U) Table 3. Array signal gain (ASG) for 120 m segments of a 600 m range interval and for the total interval. Samples were computed at three different initial ranges.

(U) A question raised in the previous paragraph is how far apart are irregularities or nulls. This depends entirely on how deep a null constitutes an irregularity. Without trying to answer the question, it appears that nulls occur about every 800 m (figure 3). This indicates that 600 m is close to the maximum interval of good correlation.

(U) Figure 7 shows propagation loss at a longer range for Site 4 and for Site 3 (Site 3 is bottom limited). The occurrence of nulls is similar in both cases. It is difficult to decide which nulls might be serious; one can estimate an average spacing of anywhere from 0.5 to 2.5 km. More work is required to determine coherence lengths.

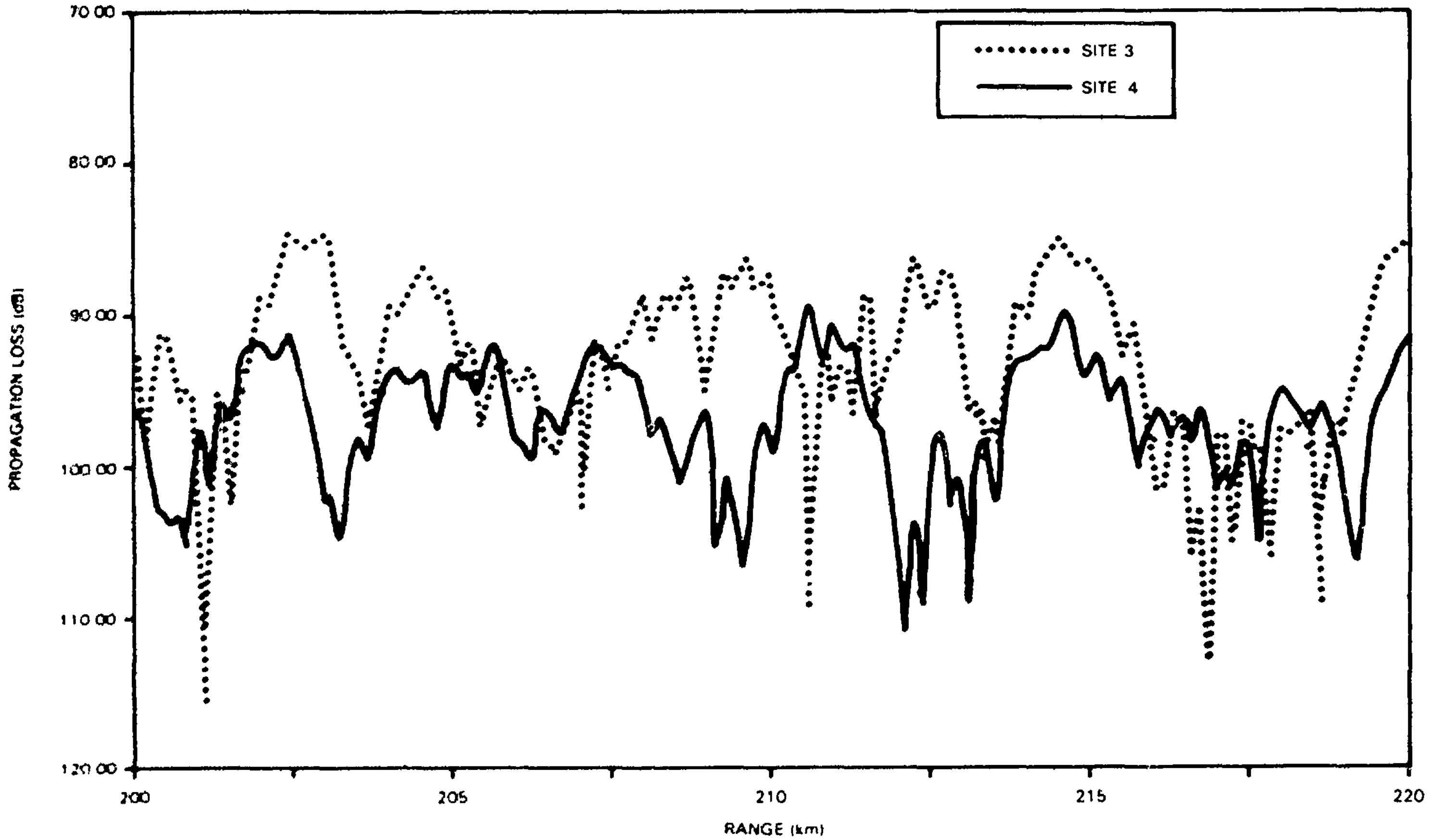

(UNCLASSIFIED)

(U) Figure 7. Propagation loss vs range computed for two sites. Source depth 80 m, receiver depth 180 m, frequency 25 Hz.

SITE 2 (U)

(C) As explained earlier, the depth sensors at Site 2 were not functioning and the tilt was unknown. However, weights had been added which were calculated to overcome the excess buoyancy and cancel the tilt. The present technique cannot model a flat array because all receivers are at the same depth and, therefore, identical; the ASG is 0 and the coherence is 1. The observed data of reference 3 suggest a conclusion regarding array tilt. The average ASG for Site 2, Tow 2PA3, is -1.66 dB. This average comes from 56 samples taken on a range from 122 to 400 km. For Site 4 the average ASG was -2.4 dB and for Site 5 it was -2.0 dB. The array tilt at Site 4 and 5 was 1.5 degrees. This suggests a loss of about 1/2 dB in ASG due to array tilt.

SITE 5 (U)

(C) Figure 8 compares the observed and modeled ASG for LATA at Site 5. The average of the observed ASG is 2.0 dB and of the modeled ASG 0.2 dB. Only 4 of the 11 modeled cases have a noticeable loss in ASG. Several others actually have a slightly positive ASG. This is possible because the ASG here is for the weighted array. Results for the unweighted array are slightly different but give the same general result.

(C) The range rate for Site 5 was only 2.2 knots because the source heading was nearly perpendicular to the direction of LATA. A sample for Site 5 covers only about half the range as did the sample for Site 4. The section on averaging time indicated that this smaller range interval could account for the improvement in ASG at Site 5 of 0.4 and 0.5 dB for the observed and simulated data, respectively, over that at Site 4.

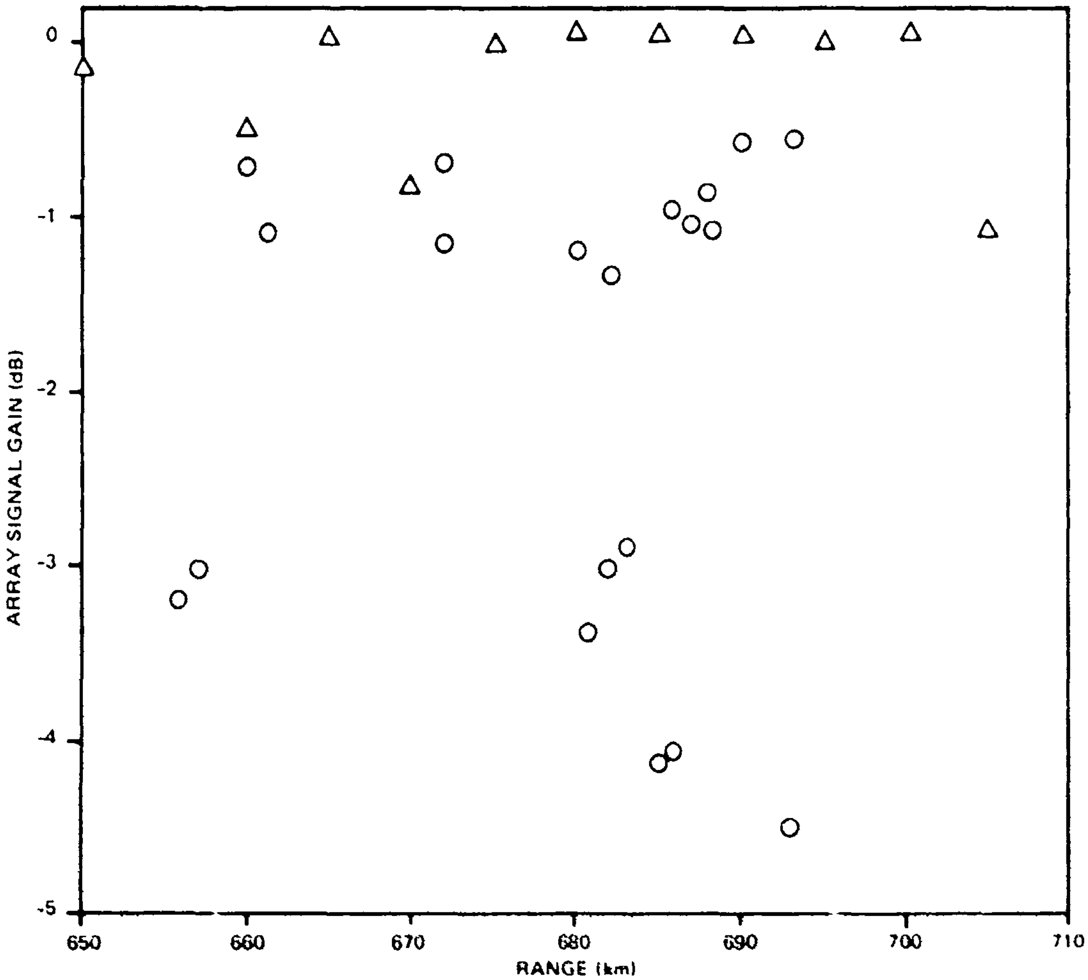

(CONFIDENTIAL)

(U) Figure 8. Array signal gain at ranges where observed data (o) and computed data (Δ) were processed for Site 5, 25 Hz, LATA. Weighted beamforming was used.

OAMS SIMULATION RESULTS (U)

(U) An array tilt of 1 degree leads to the element depths of table 1. To model Site 3 we used a range rate of 4.17 m/s or 8.1 knots. We first tried computing propagation loss each 4.17 m in range for 240 samples to provide input for the array analysis program. Next, we reduced the input to 60 samples 16.7 m apart. Since this gave essentially identical results we adopted it as our standard technique. This is equivalent to a sample every 4 seconds — the same as used for LATA.

(U) Figure 9 shows the ASG at various ranges for the observed and modeled data at Site 3. The modeled results account for almost none of the observed loss in ASG.

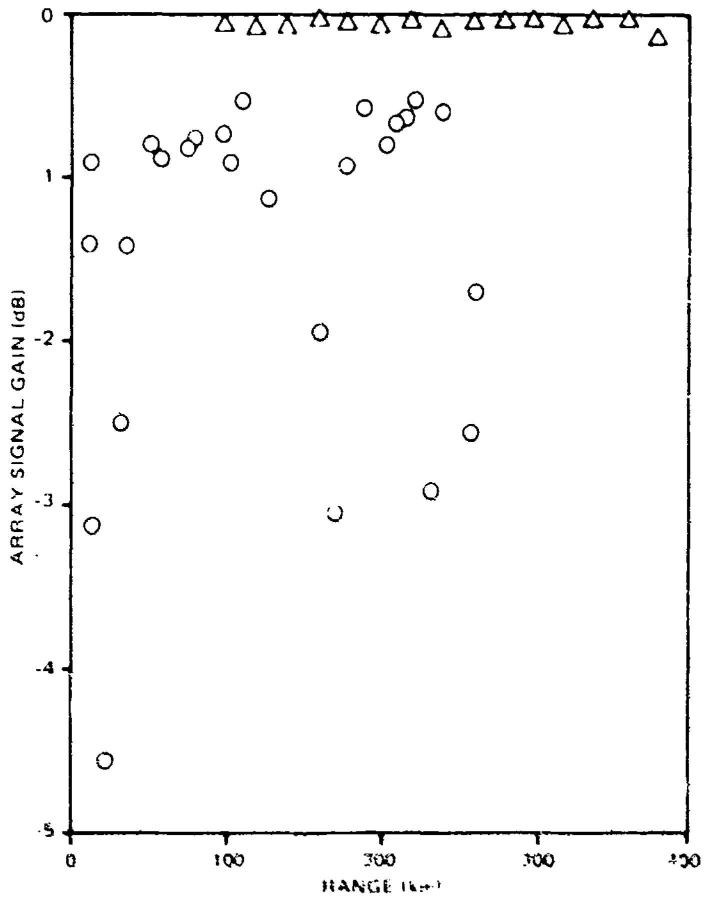

(CONFIDENTIAL)

(U) Figure 9. Array signal gain at ranges where observed data (o) and computed data (Δ) were processed for Site 3, 25 Hz, OAMS.

(C) Figure 10 shows ASG for Site 5. In these computations the same range rate as in Site 3 was used. This rate is 15 km/hr. The experimental range rates were about 17 km/hr at Site 3 and 14 km/hr at Site 5. The modeled results account for a very small part of the observed loss in ASG. This very small loss is apparently due to the vertical projection of the array being only half of that for LATA. The concentration of elements near the center of the array also, in effect, shortens it.

(C) To isolate some of the differences in our computed results for LATA and OAMS we repeated the Site 4 computations presented in figure 2 and changed only the receiver depths from those of LATA to OAMS. Instead of evenly spaced depths from 270 to 300 m we used the OAMS spacing as in table 1 from 285 to 300 m depth. We modeled the two arrays in exactly the same configuration except for the array tilt which is 1.5 degrees for LATA and 1.0 degree for OAMS.

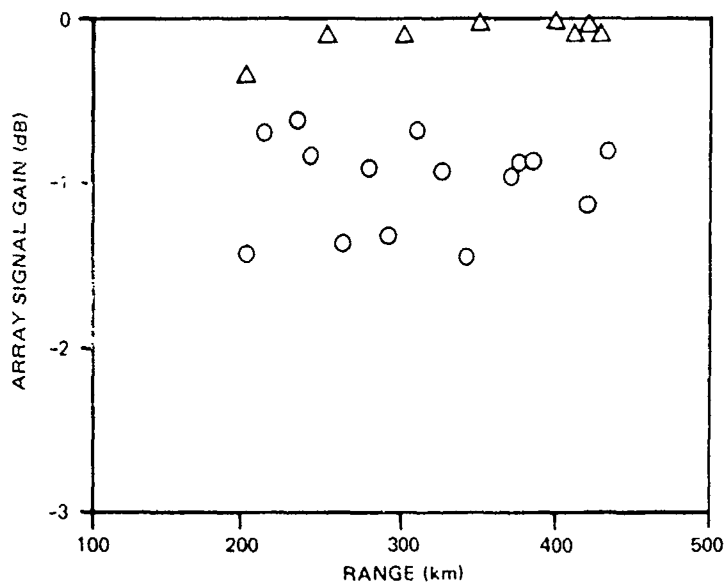

(CONFIDENTIAL)

(U) Figure 10. Array signal gain at ranges where observed (o) and computed (Δ) data were processed for Site 5, 22 Hz, OAMS.

(U) The results show that, at every range computed, OAMS suffered less loss in ASG than in LATA. The average ASG was -0.21 dB for OAMS and -0.70 dB for LATA. This is only 30 percent as much ASG loss for OAMS as for LATA. The difference of 0.5 dB is probably not detectable in the observed results because it is a small part of the total and parameters such as range rate and array depth vary.

(U) As a final comparison between OAMS and LATA we can count the number of times the ASG is less than -0.3 dB. This number roughly indicates those times when a null occurs in the field sampled by the array. Using the ASG plots of figures 2, 8, 9, and 10 and the OAMS Site 4 computations just discussed, we find in 13 cases out of 27 that LATA was less than -0.3 dB. For OAMS, only 3 in 35 were less than -0.3 dB. This indicates that the weighted spacing of OAMS makes it effectively much shorter than its true length.

COHERENCE DIAGRAM OSCILLATIONS (U)

(U) Reference 3 (pages 88-91) shows coherence diagrams for Site 4. Many of these diagrams have well defined serpentine oscillations across them. The plots were selected for their special interest. It is not stated how common the oscillations are, although one clear example from Site 2 is shown. Over a 3-hour period these sine wave-like oscillations appear to progress from about 1/2 to 3 cycles. That is, the period of the sine wave shortens and more cycles occur across the maximum element separation which is the length of the array.

(U) Figure 11 shows the above change in phase. The total phase across the coherence plots was judged by measuring the distance to each maximum or minimum of the sine wave. The extreme values of the phase when they were different are shown in the figure. A line connects those cases having the most distinct wave patterns. The three sets of open circles are curves where the 20 Hz (rather than the 25 Hz) signal was selected from the transmitted sequence of the two frequencies. If this phenomenon is interpreted as an arrival angle difference, as will be suggested later, then the three 20 Hz values can be lowered by 20 percent. If these values are lowered then a reasonably consistent line of increasing phase is seen up until 1300 hours.

(U) However, if one disregards the one high point at 1300 hours an argument could be made for a near constant line around 3π. We will assume the increasing slope of figure 11 in the following.

(U) A maneuver by the towing ship may have affected the array around 1300 hours. Figure 12 shows the target bearing obtained from the array analysis (ref 3) versus time of day. It appears that the array was probably turned through end fire in relation to the target between 1200 and 1300 hours.

(U) Figure 13 is one of the coherence plots from reference 3. The sine wave effect on it is rather confusing and it gives the double set of bars on figure 11 at 1111 hours. For completeness, figures 14 and 15 also show the array beamformer output and the average signal level at each element for the same data set.

(U) We first tried to model the effects discussed above by placing a sine wave deformation on the array. This did not work -- it will be discussed later. Adding a second signal did work and this will be described next.

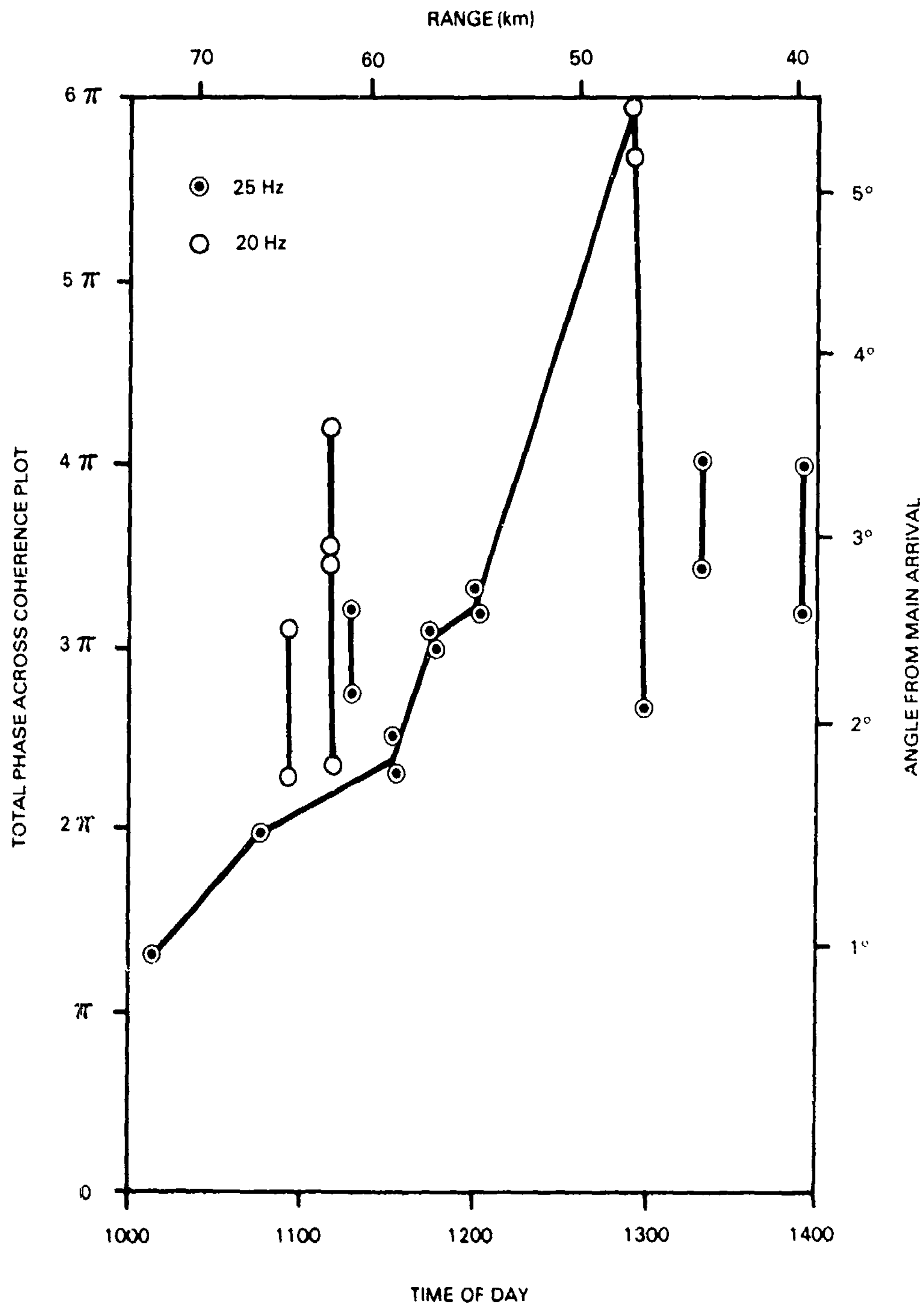

(UNCLASSIFIED)

(U) Figure 11. Total phase of the sine wave-like oscillations in the coherence plots of the observed data from Site 4, Tow 4P1. The right hand scale is the azimuthal separation between two incoherent sources that produce the equivalent total phase in this configuration.

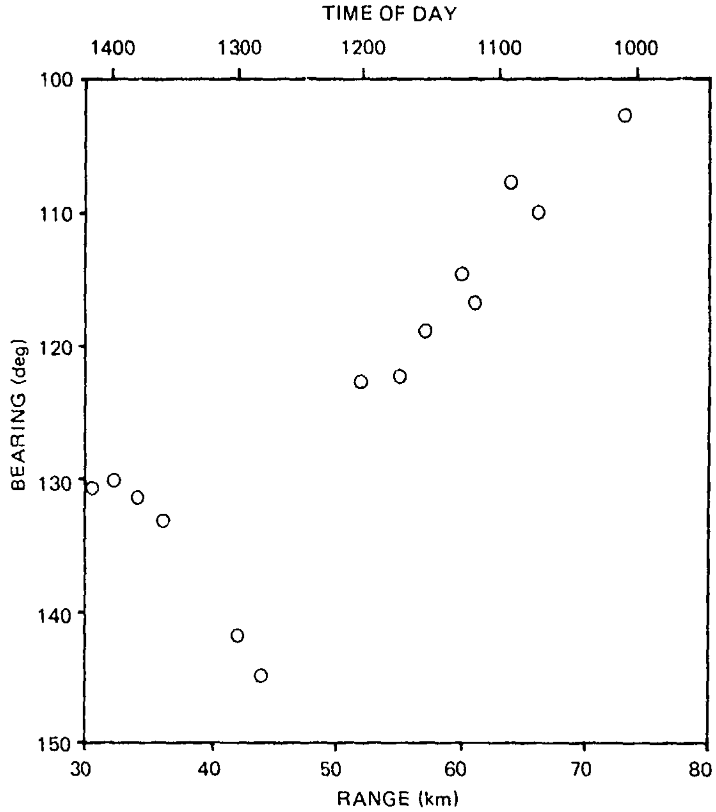

(UNCLASSIFIED)

(U) Figure 12. Bearing to the source ship as a function of range and clock time for Site 4, Tow 4P1. Bearings were determined by the array analysis program from recorded data. Bearing is measured from forward end fire.

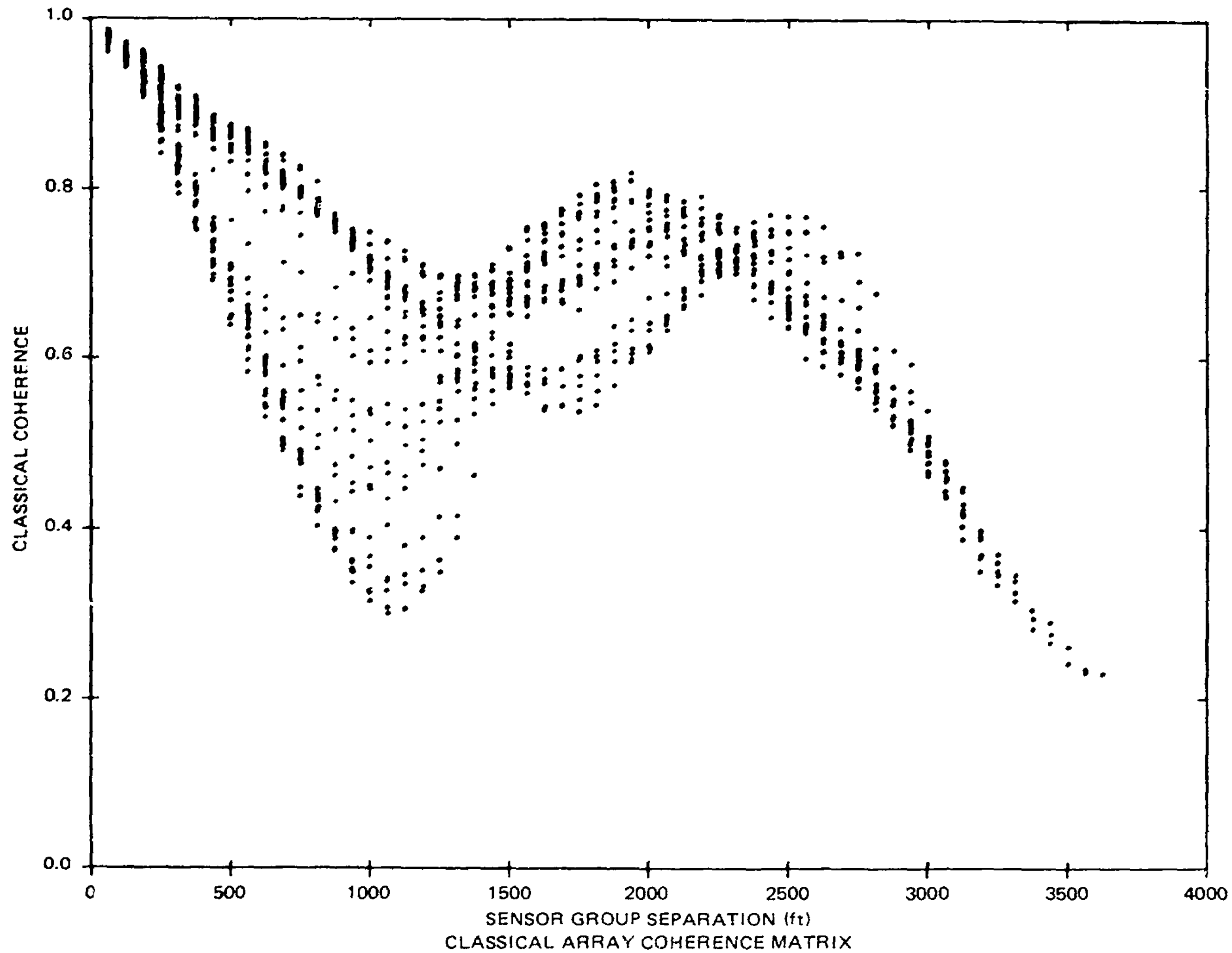

(CONFIDENTIAL)

(C) Figure 13. Coherence between pairs of elements of LATA as a function of element separation on the array. Site 4, Tow 4P1, 1111 hours.

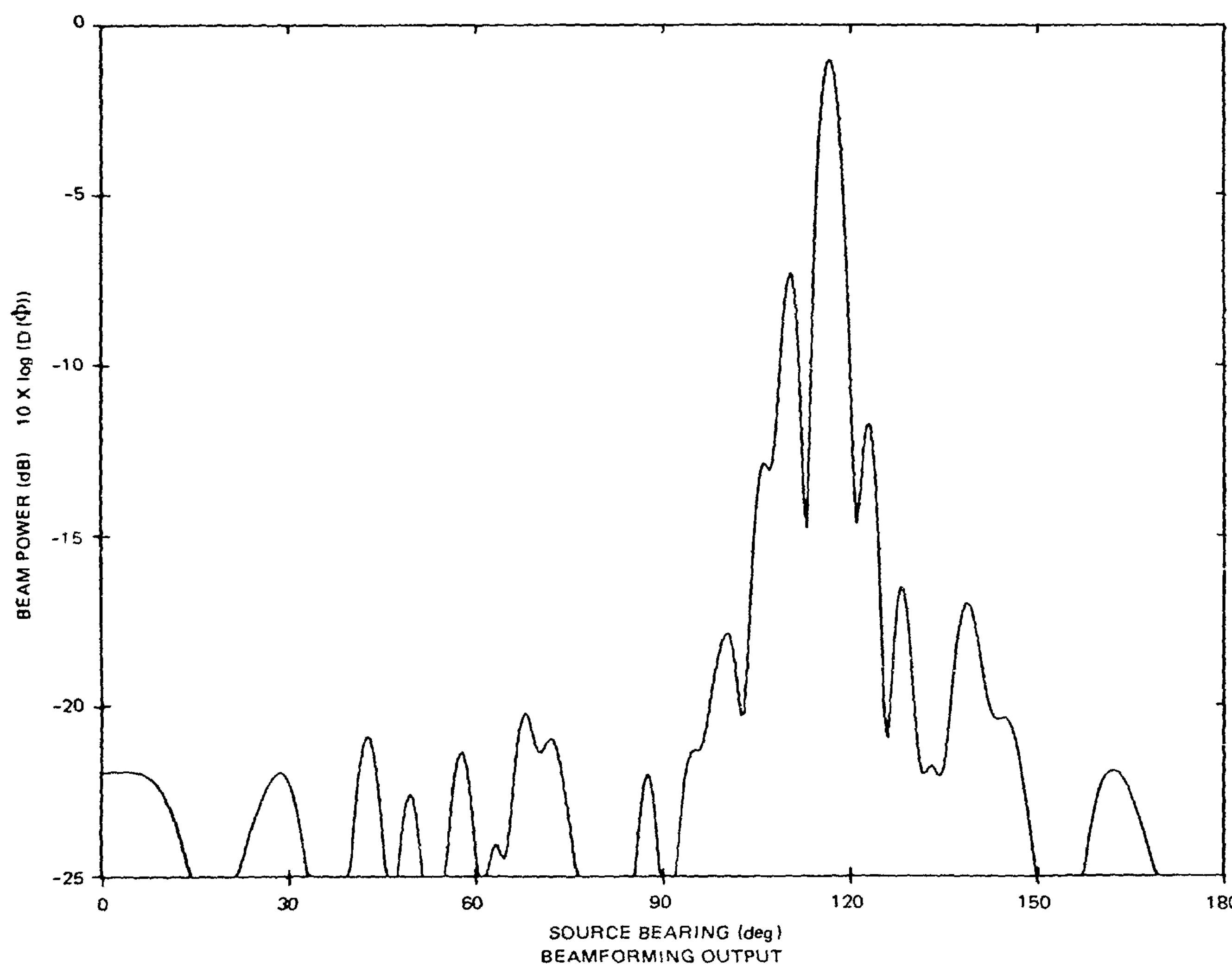

(CONFIDENTIAL)

(C) Figure 14. Beamformer output for LATA, Site 4, Tow 4P1, 1111 hours.

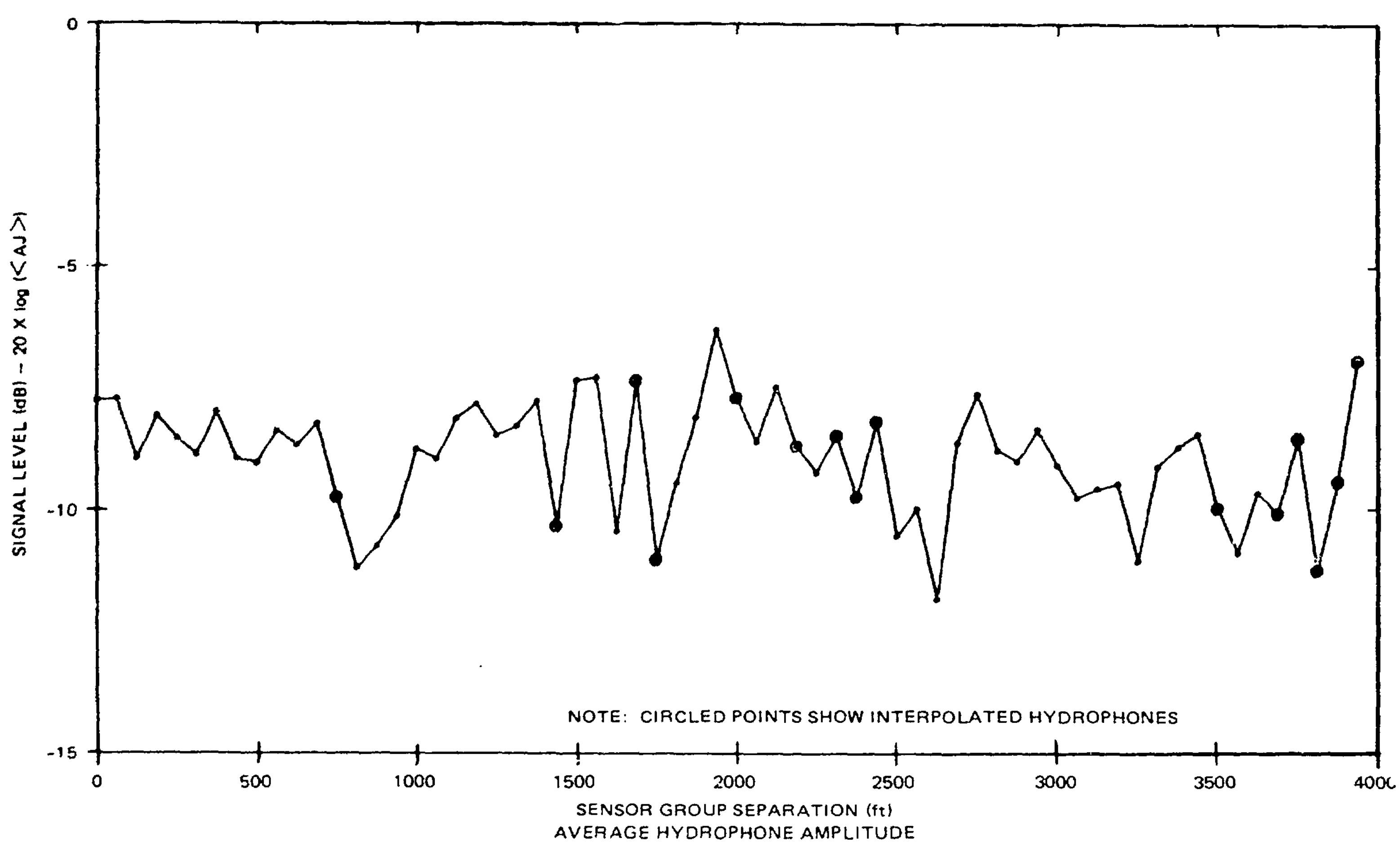

(CONFIDENTIAL)

(C) Figure 15. Average level at each element of LATA for Site 4, Tow 4P1, 1111 hours.

ADDING A SECOND SIGNAL (U)

(C) We first added a second signal to a computed sound field. A smooth case, Site 5 at 700 km, was selected. The second sound field was 10 dB less in magnitude at each field point than the first and had a phase equal to the first plus an increment. The increment increased linearly from element to element. The increase amounted to 1.5 cycles or 3π across the array. The result of this combined signal in the array analysis program is shown in figures 16 to 18. Figure 16 shows the array response to this signal as a function of steering angle. The second signal is seen 4.5 degrees from the main arrival. The array (LATA) is 19.9 wavelengths long in this water so the 1.5 cycles represent a steering of 4.3 degrees from broadside.

(U) Figure 17 shows the average signal amplitude at each array element. The effect of interference between the two signals is clearly seen. Plots of this type for the observed data, though irregular, do not show wave patterns of this amplitude (fig 17). Figure 18 shows the coherence plot and there is no sine wave on it. It is obvious that this method did not explain the sine wave effect.

(U) Realizing that adding fixed multiples of two signals to themselves should not change the coherence between them, we stopped the added signal half way through the 60 sample set. This did create the sine wave shown in figure 19. The plot of average amplitude along the array is not shown but it is predictably similar to figure 17 but with an oscillation of only one half the amplitude.

(U) This successful modeling of a sine wave in the coherence plot shows that the period of oscillation is a predictable function of the angle between the two signals and that a source of incoherence is required between the signals. Here, the intermittent nature of one signal provided the incoherence. In the observed data it is likely that two independent propagation paths could supply the incoherence.

(U) To further investigate the incoherence in the model, we added a second path that was a perfect plane wave rather than a replica of the computed signal. The plane wave was at a level of 110 dB, 14 dB below the average amplitude at all elements for the computed signal. It was again steered to gain 3π in phase across the array with the resulting phase coherence plot shown in figure 20. The sine wave effect is clearly seen. Runs with phase gain other than 3π showed that the period of the sine wave was clearly predictable and had the same total phase as the steering.

(U) A final question addressed was the effect of a null or irregularity in the computed sound field. We selected Site 5 at 660 km to be augmented by the same plane wave as above. The average amplitude plot for this case is shown in figure 21; figure 22 shows the same data plus the plane wave. A null at one end of the array brings the average amplitude there to within 1 dB of that of the added plane wave. Figure 23 shows the coherence plot for this case. Here we see a sine wave with some element pairs showing a large amplitude. The large amplitude oscillation probably results when one of the pairs is from the end of the array where the signal is small and the same size as the added plane wave.

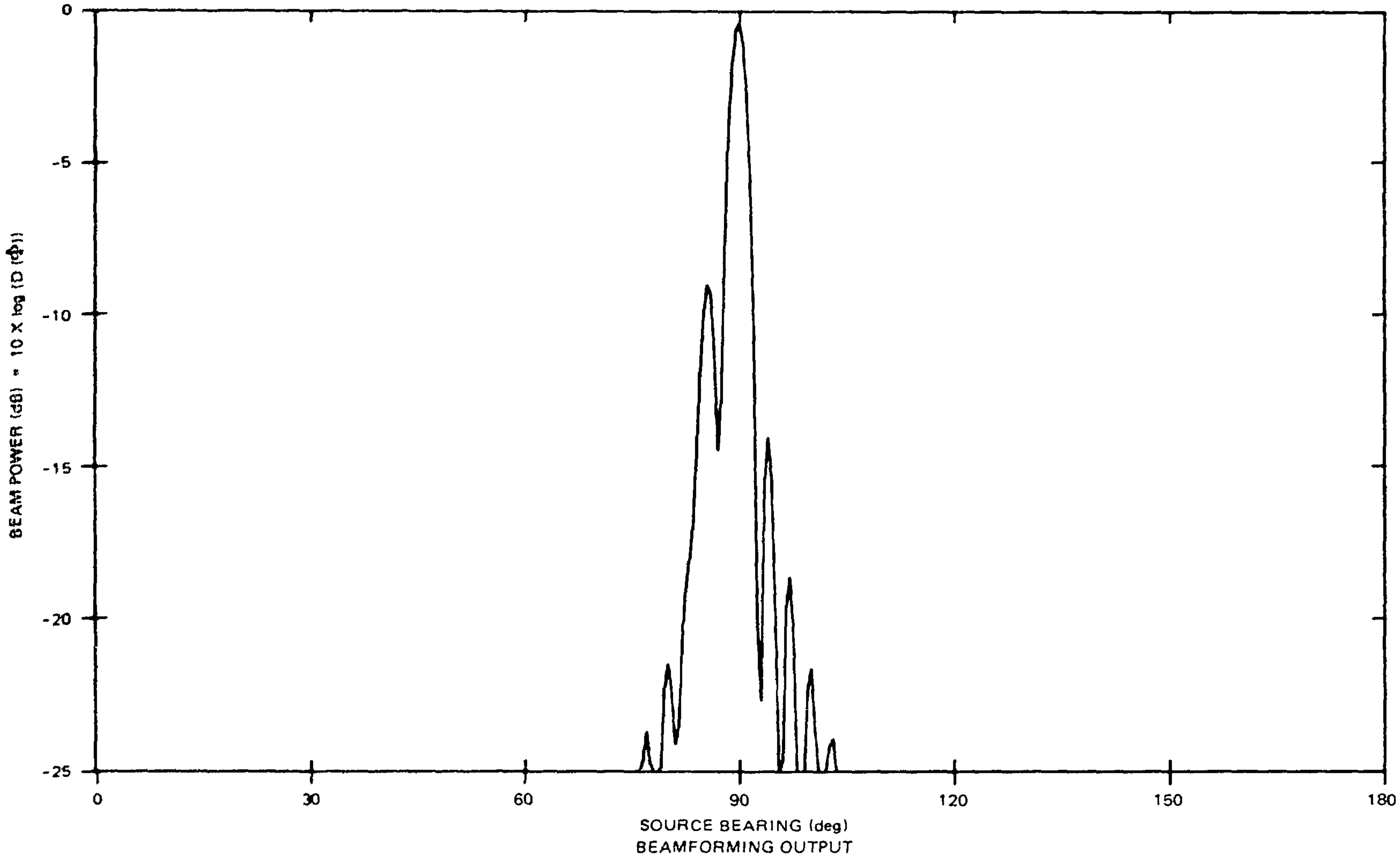

(CONFIDENTIAL)

(C) Figure 16. LATA array beam pattern for computed field to which a second source has been added by adding a component to the sound pressure at each field point which is 10 dB smaller in amplitude and progressively greater in phase by 3π across the array. Site 5, 25 Hz, 700-km range.

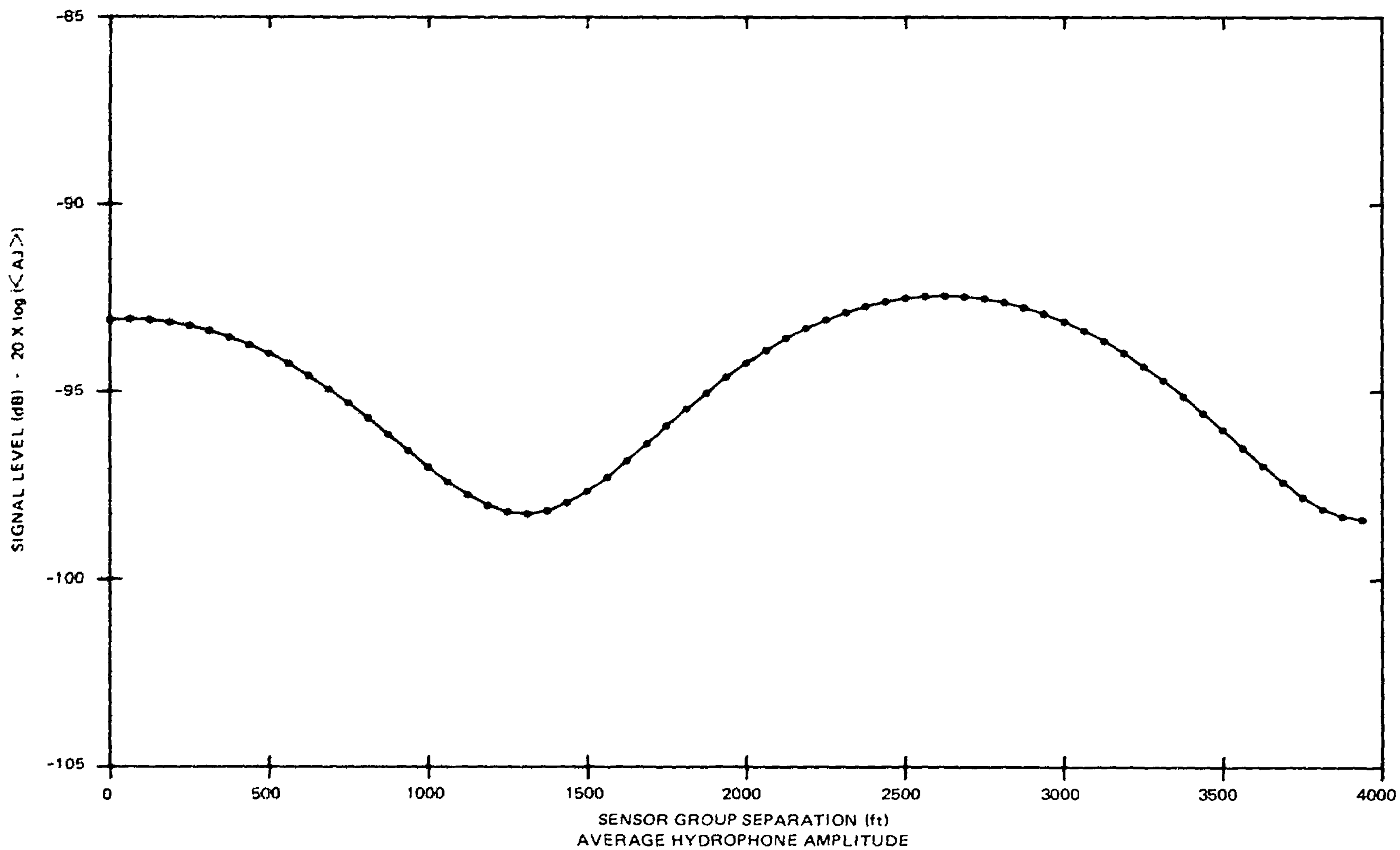

(UNCLASSIFIED)

(U) Figure 17. Average sound pressure amplitude at each array element for the same data as shown in figure 16.

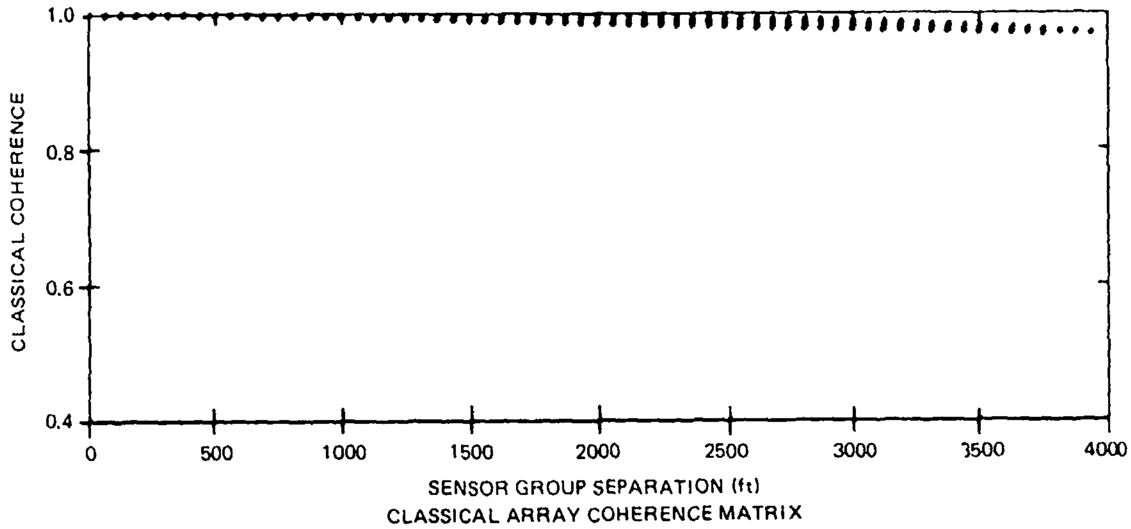

(UNCLASSIFIED)

(U) Figure 18. Coherence between array element pairs as a function of pair separation for the same data as shown in figure 16.

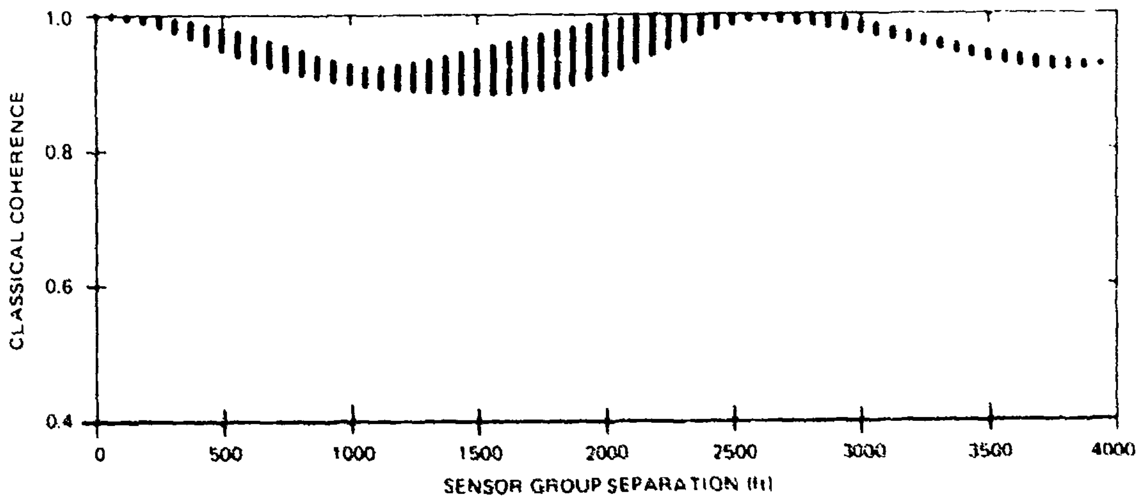

(UNCLASSIFIED)

(U) Figure 19. Coherence between array element pairs as a function of pair separation for the same data as shown in figure 18 except that the second signal is added to the first 30 range samples but not the last 30.

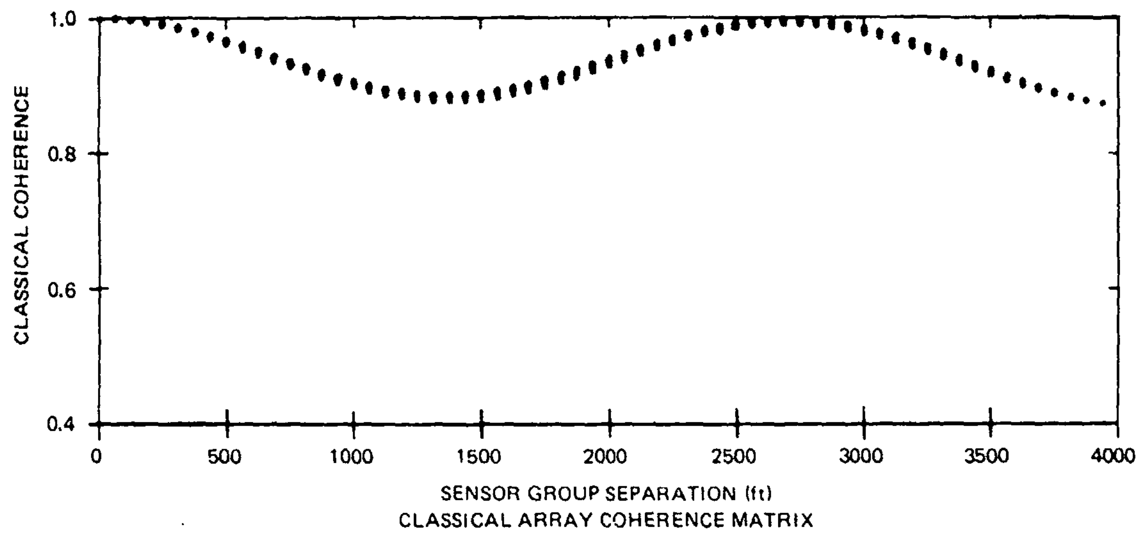

(UNCLASSIFIED)

(U) Figure 20. Coherence between element pairs for the computed sound field for Site 5, 25 Hz, 700 km range. A second signal which is a plane wave of 110 dB propagation loss arrives at an angle which results in a 3 phase advance across the array.

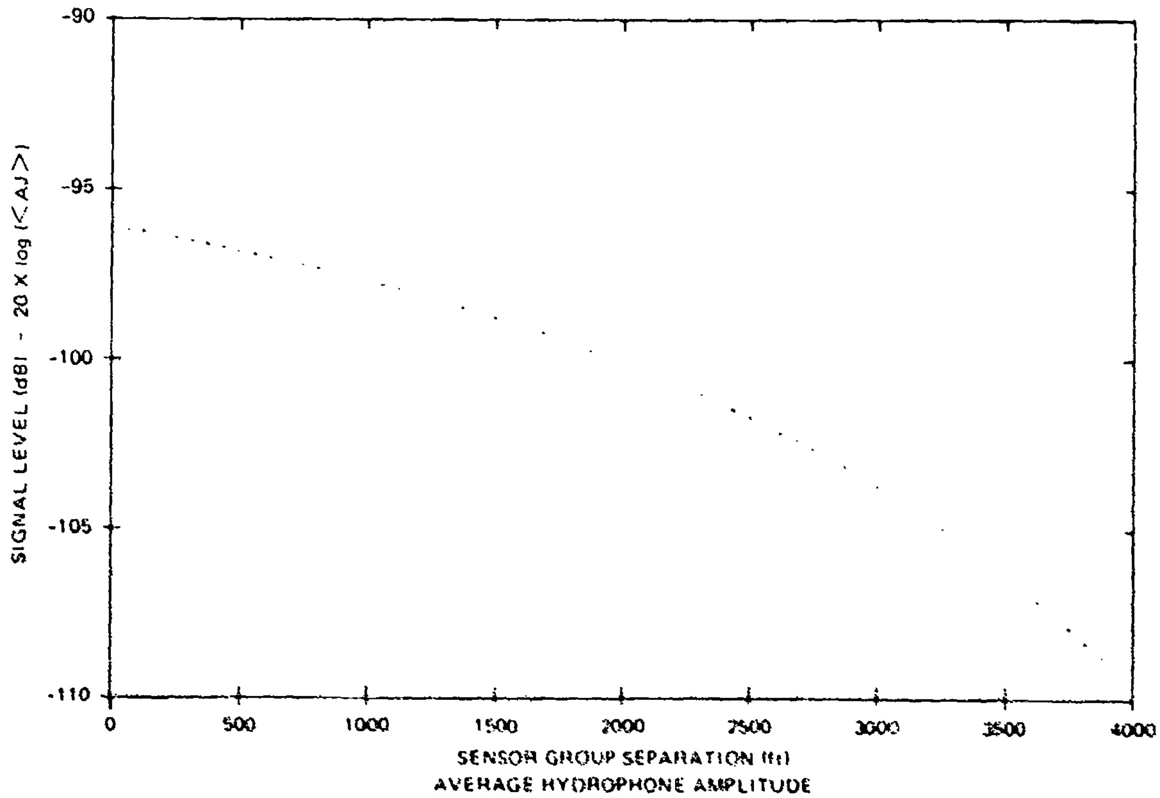

(UNCLASSIFIED)

(U) Figure 21. Average sound pressure amplitude at each array element for a computed sound field for Site 5, 25 Hz, range 660 km. This range was selected because of its irregular field.

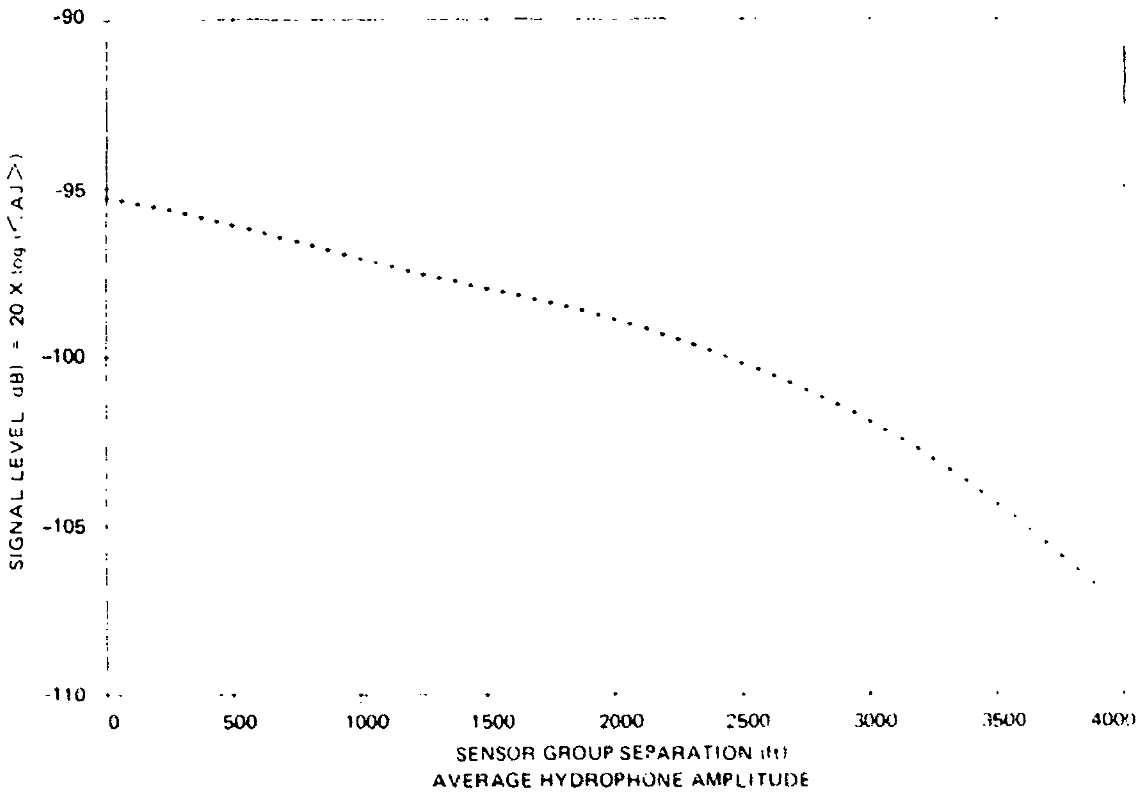

(UNCLASSIFIED)

(U) Figure 22. Average sound pressure amplitude at each array element for the computed sound field for Site 5, 25 Hz, 660 km range plus a second plane wave arrival as shown in figure 20.

(U) These results show that the presence of a second signal is a plausible explanation for the sine waves in the coherence plots. We can, therefore, return to figure 11 and add an angular arrival difference scale. To do so we note from figure 12 that during the time interval from 1000 to 1300, the bearing to the target (from end fire) increased from 102 to 140 degrees. With this increase and assuming that the steering phase gain is equivalent to the total sine wave phase in the coherence plot, the angular separation scale on the right hand side of figure 11 can be determined. This tells us that the separation between the two signals increased from 1 to 4 degrees from 1000 to 1300 hours. If the second signal were an echo off a seamount or a noisy ship, then the minimum distance between it and the source would increase from 1.2 to 3.5 km over this time interval.

(U) Returning to figure 14 (from the data at 1111 hours) we see a second arrival 7 dB below the main arrival and separated from it by 6.4 degrees. This does not agree with our prediction of a 2 degree separation but it does support the idea of a second arrival. The second arrival peak in the figure is undoubtedly affected by the first sidelobe of the main arrival.

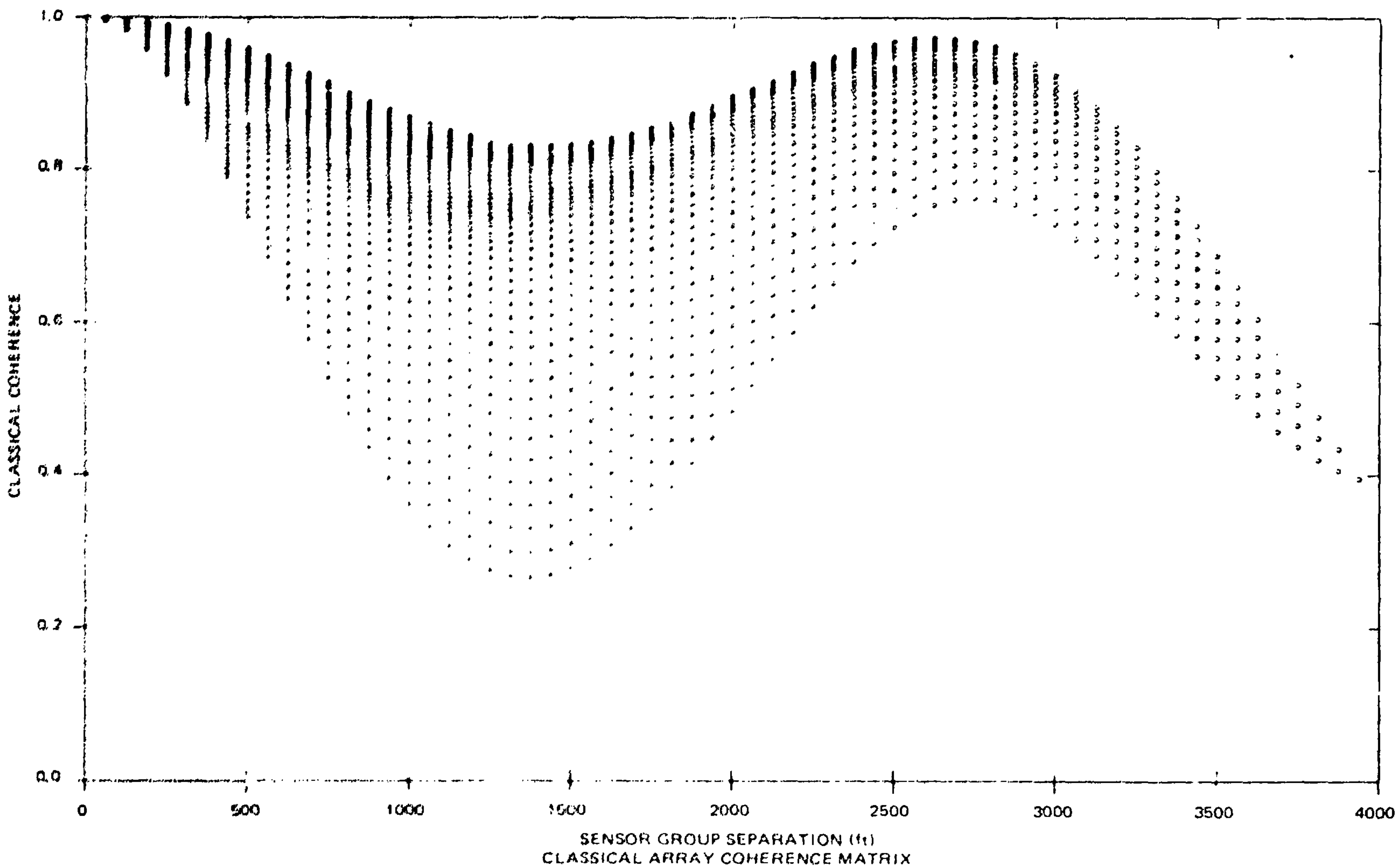

(UNCLASSIFIED)

(U) Figure 23. Coherence between element pairs for the composite sound field of figure 22.

(C) An alternative explanation of the sine wave effect is two incoherent arrivals from the same direction but of different frequencies. The arrivals must be from off broadside to be separated by the beamformer. We can compute the frequency difference required to produce the total phase of figure 11. Between 1030 and 1300 the target bearing increased from 10 to 35 degrees off broadside while the total phase from the plot increased from 1.5 to 4π. From this we find a frequency difference of 4.4 to 5.2 Hz. The two transmitted frequencies of 20 and 25 Hz could be a source of the differences. However, it is unlikely that the experimental and sampling techniques would mix the two.

ARRAY DEFORMATION (U)

(U) Array deformation was modeled in an attempt to explain the oscillations in the coherence plots (ref 3). We modeled vertical and horizontal sine wave displacements of the array elements of amplitudes up to 1 and 4 m. No evidence of sine waves in the coherence plots was found. This is the principal result. A second result is the decrease in ASG caused by these deformations. We will outline the modeling method and report the ASG losses in the text to follow.

(C) To model displacement we assumed that a sine wave of given total phase existed along the array at the beginning of the 4 minute sample. We then assumed that this sine wave moved along the array at the tow speed of 3 knots or 1.54 m/s. Thus, a point on the sine wave traveled down the array almost one third of its length during the 4 minute sampling. The computed sound field consists of pressures at a matrix of 60 range points and 64 depth points. A horizontal displacement is modeled by interpolating between range points and a vertical displacement is modeled by interpolating between depth points. Both phase and amplitude of pressure are interpolated. With acoustic wavelengths of 60 m and displacements no greater than 4 m, linear interpolation is permissible. The input to the array analysis program is, thus, a set of pressures at 60 consecutive ranges which have been altered slightly in amplitude and phase to represent a sine wave progressing along the array.

(U) Two different initial sound fields were used — a smooth case, Site 5 at 700 km and an irregular case, Site 5 at 660 km. Table 4 shows the ASG resulting from these two cases. Loss in ASG can be determined by comparison to the zero amplitude entries. The table shows that, with one exception, deforming the array decreases the ASG. The exception to this is that the last entry for the weighted array increased from -0.500 to -0.112 dB. We suspect that the deformation by chance canceled an irregularity in the field. Although all other cases decrease, the decrease is small and never greater than 0.5 dB. There is little difference in the decrease for the 700 and 660 km cases. These results support the obvious conclusion that deformation of the array will decrease the ASG. The amount of deformation modeled here has a minimal adverse effect on the ASG.

(U) For completeness, the ASG for the two arrival cases discussed at the beginning of this section is given in table 5. The first entry for each range is again the unperturbed case for comparison. In the first of these a second arrival of 10 dB down was added, the phase was not altered, and the identical

ASG, to the unaltered case was obtained as a check. In all other cases the adding of a second wave decreased the ASG. The decreases range from 0.12 to 0.38 dB with one large decrease of 1.49 dB. As was the case in table 4, the ASG changes are highly variable. There is a question here as to whether the effect of a second signal should be interpreted as a loss in signal gain or in noise gain. Since noise gain is not addressed in this report, we have called it signal gain in order to compare it to other cases.

Range (km)	Sine Wave Amplitude (m)	Sine Wave Total Phase (radians)	Vertical or Horizontal	ASG Weighted (dB)	ASG Unweighted (dB)
700	0	-	-	+0.080	-0.008
700	1.0	1.0π	h	+0.076	-0.010
700	1.0	2.5π	h	+0.065	-0.031
700	4.0	2.5π	h	-0.155	-0.352
700	1.0	2.5π	v	+0.065	-0.060
660	0	-	-	-0.500	-0.605
660	4.0	2.5π	h	-0.623	-0.784
660	1.0	2.5π	v	-0.112	-0.737

(UNCLASSIFIED)

(U) Table 4. ASG for sine wave deformation of the array.

Range (km)	Added Wave Amplitude (m)	Added Wave Phase (radians)	Description	ASG Weighted (dB)	ASG Unweighted (dB)
700	10 dB down	0	Replica	+0.080	-0.008
700	10 dB down	2π	Replica	-1.405	-0.290
700	10 dB down	3π	Replica	-0.303	-0.391
700	10 dB down	3π	Intermittent	-0.142	-0.237
700	-110 dB total	3π	Plane wave	-0.098	-0.132
660	0		none	-0.500	-0.605
660	-110 dB total	3π	Plane wave	-0.679	-0.812

(UNCLASSIFIED)

(U) Table 5. ASG for added second arrival.

CONCLUSIONS (U)

(U) A deterministic sound field computed from idealized boundary conditions has been used in the place of real data in Dr JA Neubert's array analysis program. The following were developed from the analysis:

1. (U) The computed field modeled two parameters of the observed field – multipath propagation and differing element depths arising from array tilt. This model accounted for between 10 and 25 percent of the loss in ASG for LATA, but almost none for OAMS which had about one half the vertical projection of LATA. The remaining loss in ASG may arise from the horizontal projection of the array in the multipath field, noise interference, array deformation, malfunction of array elements, and fluctuations.

2. (U) Plots of average amplitude and of coherence between array elements differed for the modeled and observed data in that those for the modeled data had a high degree of regularity which was lacking in the observed data. However, similar overall shape was observed for both.

3. (U) Modeling showed that array deformations of up to 4 m gave losses in ASG but the losses were not great enough to explain the difference between observed and modeled ASG.

4. (U) The particular Bearing Stake sites had no large or apparent differences in their effects on the modeled ASG and coherence. More repetitions with more nearly identical parameters would have to be computed to obtain statistically significant comparisons.

5. (U) Losses in ASG can be correlated with the presence of nulls in the computed sound field. Significant losses were encountered in 50 percent of the sample sets for LATA but in less than 10 percent for OAMS.

6. (U) Serpentine oscillations in the element pair coherence plots can be modeled by adding a second source at a small bearing separation from the first. The second must not be fully coherent with the first. This was modeled by making the second source intermittent and by making it an ideal plane wave. In the observed data an echo from an object or a noise source near the signal source could provide these requirements.

REFERENCES (U)

1. Naval Ocean Systems Center TR 383, "Bearing Stake Coherence and Array Signal Gain Area Assessment Report (U)" by JA Neubert, Confidential, December 1978

2. Naval Ocean Systems Center TN 380, "Bearing Stake Coherence Data Analysis, OAMS Array (U)" by JA Neubert, Confidential, 6 February 1978*

3. Naval Ocean Systems Center TN 589, "Bearing Stake Coherence Data Analysis: LATA (U)" by AG Fabula and JA Neubert, Confidential, December 1978*

4. JA Neubert, "Coherence and Its Sound Field Structure in the Northwestern Indian Ocean (U)," JUA(USN) 30(3), p 367-398 Confidential, 1980

5. Naval Ocean Systems Center TR 467, "Propagation Loss Assessment of the Bearing Stake Exercise (U)," by MA Pederson and GS Yee, Confidential, September 1979

6. DF Gordon and ER Floyd, "Acoustic Propagation Effects in Beam Forming of Long Arrays (U)," JUA(USN) 29(1), p 1-16, Confidential, January 1979

7. Naval Ocean Systems Center TR 393, "Underwater Sound Propagation-Loss Program, Computation by Normal Modes for Layered Oceans and Sediments," by DF Gordon, Unclassified, May 1979

8. NORDA Report 18, "Bearing Stake Exercise: Sound Speed and Other Environmental Variability (U)," by DF Fenner and WJ Cronin, Jr, Confidential, September 1978

9. ARL-TR-79-24, "Analysis of Acoustic Bottom Interaction in Bearing Stake (U)" by SK Mitchell and others, Confidential, February 1979

*NOSC Technical Notes are informal publications intended primarily for use in the Center.

DISTRIBUTION LIST (U)

COMMANDER
NAVAL ELECTRONIC SYSTEMS COMMAND
WASHINGTON, DC 20360
ATTN: CODE 3203 (R. MITNICK)
320A (J.A. SINSKY)
PME 124 (CAPT H. COX)
124TA (R. KNUDSEN)

COMMANDER
NAVAL SEA SYSTEMS COMMAND
WASHINGTON, DC 20362
ATTN: A.P. FRANCESCHETTI

CHIEF OF NAVAL RESEARCH
800 N. QUINCY ST
ARLINGTON, VA 22217

CHIEF OF NAVAL MATERIAL
NAVY DEPARTMENT
WASHINGTON, DC 20360
ATTN: NAVMAT 08D1, (CAPT E. YOUNG)

COMMANDING OFFICER
NAVAL OCEAN RESEARCH AND DEVELOPMENT ACTIVITY
NSTL STATION, MS 39529
ATTN: CODE 500
300
LIBRARY

COMMANDING OFFICER
U.S. NAVAL OCEANOGRAPHIC OFFICER
NSTL STATION
BAY ST. LOUIS, MS 39522
ATTN: CODE 7000, (W. GEDDES)

SUPERINTENDENT
NAVAL POSTGRADUATE SCHOOL
MONTEREY, CA 93940
ATTN: LIBRARY

DEFENSE ADVANCED RESEARCH PROJECT AGENCY
1400 WILSON BLVD.
ARLINGTON, VA 22209

ARPA RESEARCH CENTER
UNIT 1, BLDG. 301A
NAS MOFFETT FIELD, CA 94035
ATTN: E.L. SMITH

APPLIED RESEARCH LABORATORIES
UNIVERSITY OF TEXAS
P.O. BOX 8029
AUSTIN, TX 78712
ATTN: LIBRARY

APPLIED PHYSICS LABORATORY
JOHNS HOPKINS UNIVERSITY
JOHNS HOPKINS ROAD
LAUREL, MD 20810
ATTN: LIBRARY

MARINE PHYSICAL LABORATORY
UNIVERSITY OF CALIFORNIA, SAN DIEGO
SAN DIEGO, CA 92152
ATTN: LIBRARY

WOODS HOLE OCEANOGRAPHIC INSTITUTION
WOODS HOLE, MA 02543
ATTN: LIBRARY

[This page is unclassified]

DEPARTMENT OF THE NAVY
OFFICE OF NAVAL RESEARCH
875 NORTH RANDOLPH STREET
SUITE 1425
ARLINGTON VA 22203-1995

IN REPLY REFER TO:

5510/1
Ser 321OA/011/06
31 Jan 06

MEMORANDUM FOR DISTRIBUTION LIST

Subj: DECLASSIFICATION OF LONG RANGE ACOUSTIC PROPAGATION PROJECT (LRAPP) DOCUMENTS

Ref: (a) SECNAVINST 5510.36

Encl: (1) List of DECLASSIFIED LRAPP Documents

1. In accordance with reference (a), a declassification review has been conducted on a number of classified LRAPP documents.

2. The LRAPP documents listed in enclosure (1) have been downgraded to UNCLASSIFIED and have been approved for public release. These documents should be remarked as follows:

    Classification changed to UNCLASSIFIED by authority of the Chief of Naval Operations (N772) letter N772A/6U875630, 20 January 2006.

    DISTRIBUTION STATEMENT A: Approved for Public Release; Distribution is unlimited.

3. Questions may be directed to the undersigned on (703) 696-4619, DSN 426-4619.

BRIAN LINK
By direction

Subj: DECLASSIFICATION OF LONG RANGE ACOUSTIC PROPAGATION PROJECT (LRAPP) DOCUMENTS

DISTRIBUTION LIST:

NAVOCEANO (Code N121LC – Jaime Ratliff)
NRL Washington (Code 5596.3 – Mary Templeman)
PEO LMW Det San Diego (PMS 181)
DTIC-OCQ (Larry Downing)
ARL, U of Texas
Blue Sea Corporation (Dr.Roy Gaul)
ONR 32B (CAPT Paul Stewart)
ONR 321OA (Dr. Ellen Livingston)
APL, U of Washington
APL, Johns Hopkins University
ARL, Penn State University
MPL of Scripps Institution of Oceanography
WHOI
NAVSEA
NAVAIR
NUWC
SAIC

Declassified LRAPP Documents

Report Number	Personal Author	Title	Publication Source (Originator)	Pub. Date	Current Availability	Class.
ARLTR7952	Focke, K. C., et al.	CHURCH STROKE 2 CRUISE 5 PAR/ACODAC ENVIRONMENTAL ACOUSTIC MEASUREMENTS AND ANALYSIS (U)	University of Texas, Applied Research Laboratories	791029	ADC025102; NS; AU; ND	C
Unavailable	Van Wyckhouse, R. J.	SYNBAPS. VOLUME I. DATA BASE SOURCES AND DATA PREPARATION	Naval Ocean R&D Activity	791201	ADC025193	C
NORDATN63	Brunson, B. A., et al.	ENVIRONMENTAL EFFECTS ON LOW FREQUENCY TRANSMISSION LOSS IN THE GULF OF MEXICO (U)	Naval Ocean R&D Activity	800901	ADC029543; ND	C
NORDATN80C	Gereben, I. B.	ACOUSTIC SIGNAL CHARACTERISTICS MEASURED WITH THE LAMBDA III DURING CHURCH STROKE III (U)	Naval Ocean R&D Activity	800915	ADC023527; NS; AU; ND	C
NOSCTR664	Gordon, D. F.	ARRAY SIMULATION AT THE BEARING STAKE SITES	Naval Ocean Systems Center	810401	ADC025992; NS; AU; ND	C
NOSCTR703	Gordon, D. F.	NORMAL MODE ANALYSIS OF PROPAGATION LOSS AT THE BEARING STAKE SITES (U)	Naval Ocean Systems Center	810801	ADC026872; NS; AU; ND	C
NOSCTR680	Neubert, J. A.	COHERENCE VARIABILITY OF ARRAYS DURING BEARING STAKE (U)	Naval Ocean Systems Center	810801	ADC028075; NS; ND	C
HSECO735	Luehrmann, W. H.	SQUARE DEAL R/V SEISMIC EXPLORER FIELD OPERATIONS REPORT (U)	Seismic Engineering Co.	731121	AD0530744; NS; ND	C; U
MPL-C-42/76	Morris, G. B.	CHURCH ANCHOR EXPLOSIVE SOURCE (SUS) PROPAGATION MEASUREMENTS FROM R/P FLIP (U)	Marine Physical Laboratory	760701	ADC010072; AU; ND	C; U
ARLTR7637	Mitchell, S. K., et al.	SQUARE DEAL EXPLOSIVE SOURCE (SUS) PROPAGATION MEASUREMENTS. (U)	University of Texas, Applied Research Laboratories	760719	ADC014196; NS; AU; ND	C; U
NORDAR23	Fenner, D. F.	SOUND SPEED STRUCTURE OF THE NORTHEAST ATLANTIC OCEAN IN SUMMER 1973 DURING THE	Naval Ocean R&D Activity	800301	ADC029546; NS; ND	C; U
NOOTR230	Bucca, P. J.	SOUND VELOCITY CONDITIONS DURING THE CHURCH ANCHOR EXERCISE (U)	Naval Oceanographic Office	751201	NS; AU; ND	C;U
ONR SP 2-69; MC PLAN-01	Unavailable	PARKA II EXPERIMENT UTILIZING SEA SPIDER, ONR SCIENTIFIC PLAN 2-69 (U)	Maury Center for Ocean Science	690626	ADB020846; ND	U
Unavailable	Unavailable	PARKA I EXPERIMENT	Maury Center for Ocean Science	691101	AD0506209	U
USRD CR 3105	Unavailable	SEA SPIDER TRANSPONDER TRANSDUCER	Naval Research Laboratory	700505	ND	U
MC PLAN 05; ONR Scientific Plan 1-71	Unavailable	ATLANTIC TEST BED MEASUREMENT PROGRAM (U)	Maury Center for Ocean Science	701020	ND	U
ACR-170 VOL.1	Hurdle, B. G.	PROJECT NEAT- A COLLABORATIVE LONG RANGE PROPAGATION EXPERIMENT IN THE NORTHEAST ATLANTIC, PART I (U)	Naval Research Laboratory	701118	ND	U
MC-003-VOL-2	Unavailable	THE PARKA I EXPERIMENT. APPENDICES- PACIFIC ACOUSTIC RESEARCH KANEOHE-ALASKA (U)	Maury Center for Ocean Science	710101	ND	U